PHYSICAL REVIEW D **83,** 112004 (2011)

Upsilon production cross section in pp collisions at $\sqrt{s} = 7$ TeV

V. Khachatryan *et al.**
(CMS Collaboration)

(Received 27 December 2010; published 15 June 2011)

The $\Upsilon(1S)$, $\Upsilon(2S)$, and $\Upsilon(3S)$ production cross sections in proton-proton collisions at $\sqrt{s} = 7$ TeV are measured using a data sample collected with the CMS detector at the LHC, corresponding to an integrated luminosity of 3.1 ± 0.3 pb^{-1}. Integrated over the rapidity range $|y| < 2$, we find the product of the $\Upsilon(1S)$ production cross section and branching fraction to dimuons to be $\sigma(pp \to \Upsilon(1S)X) \cdot \mathcal{B}(\Upsilon(1S) \to \mu^+\mu^-) = 7.37 \pm 0.13^{+0.61}_{-0.42} \pm 0.81$ nb, where the first uncertainty is statistical, the second is systematic, and the third is associated with the estimation of the integrated luminosity of the data sample. This cross section is obtained assuming unpolarized $\Upsilon(1S)$ production. With the assumption of fully transverse or fully longitudinal production polarization, the measured cross section changes by about 20%. We also report the measurement of the $\Upsilon(1S)$, $\Upsilon(2S)$, and $\Upsilon(3S)$ differential cross sections as a function of transverse momentum and rapidity.

DOI: 10.1103/PhysRevD.83.112004 PACS numbers: 13.85.Ni, 14.40.Pq

I. INTRODUCTION

The hadroproduction of quarkonia is not understood. None of the existing theories successfully reproduces both the differential cross section and the polarization measurements of charmonium and bottomonium states [1]. It is expected that studying quarkonium hadroproduction at higher center-of-mass energies and over a wider rapidity range will facilitate significant improvements in our understanding. Measurements of the Υ resonances are particularly important since the theoretical calculations are more robust than for the charmonium family due to the heavy bottom quark and the absence of b-hadron feed-down. Measurements of quarkonium hadroproduction cross sections and production polarizations made at the Large Hadron Collider (LHC) will allow important tests of several alternative theoretical approaches. These include nonrelativistic QCD (NRQCD) factorization [2], where quarkonium production includes color-octet components, and calculations made in the color-singlet model including next-to-leading-order (NLO) corrections [3] which reproduce the differential cross sections measured at the Tevatron experiments [4,5] without requiring a significant color-octet contribution.

This paper presents the first measurement of the $\Upsilon(1S)$, $\Upsilon(2S)$, and $\Upsilon(3S)$ production cross sections in proton-proton collisions at $\sqrt{s} = 7$ TeV, using data recorded by the Compact Muon Solenoid (CMS) experiment between April and September 2010. In these measurements, the signal efficiencies are determined with data. Consequently, Monte Carlo simulation is used only in the evaluation of the geometric and kinematic acceptances. The document is organized as follows. Sec. II contains a short description of the CMS detector. Sec. III presents the data collection, the trigger and offline event selections, the reconstruction of the Υ resonances, and the Monte Carlo simulation. Throughout this paper, Υ and $\Upsilon(nS)$ are used to denote the $\Upsilon(1S)$, $\Upsilon(2S)$, and $\Upsilon(3S)$ resonances. The detector acceptance and the efficiency to reconstruct Υ resonances that decay to two muons in CMS are discussed in Secs. IV and V, respectively. In Sec. VI the fitting technique employed to extract the cross section is presented. The evaluation of systematic uncertainties on the measurements is described in Sec. VII. Sec. VIII presents the $\Upsilon(nS)$ cross section results and comparisons to existing measurements at lower collision energies [4,5] and to the predictions of the PYTHIA [6] event generator.

II. THE CMS DETECTOR

The central feature of the CMS apparatus is a superconducting solenoid, of 6 m inner diameter, providing a field of 3.8 T. Inside the solenoid in order of increasing distance from the interaction point are the silicon tracker, the crystal electromagnetic calorimeter, and the brass/scintillator hadron calorimeter. Muons are detected by three types of gas-ionization detectors embedded in the steel return yoke: drift tubes (DT), cathode strip chambers (CSC), and resistive plate chambers (RPC). The muon measurement covers the pseudorapidity range $|\eta| < 2.4$, where $\eta = -\ln[\tan(\theta/2)]$ and the polar angle θ is measured from the z-axis, which points along the counterclockwise beam direction. The silicon tracker consists of pixel detectors (three barrel layers and two forward disks on either side of the detector, comprising 66×10^6 100×150 μm^2 pixels) followed by microstrip detectors (ten barrel layers plus three inner disks and nine forward disks on either side of the detector, with 10×10^6 strips of

*Full author list given at the end of the article.

Published by the American Physical Society under the terms of the Creative Commons Attribution 3.0 License. Further distribution of this work must maintain attribution to the author(s) and the published article's title, journal citation, and DOI.

 © 2011 CERN, for the CMS Collaboration

pitch between 80 and 184 μm). The detector systems are aligned and calibrated using LHC collision data and cosmic-ray muons [7]. Because of the strong magnetic field and the fine granularity of the silicon tracker, the muon transverse-momentum measurement, p_{T}, based on information from the silicon tracker alone has a resolution of about 1% for a typical muon in this analysis. The silicon tracker provides the primary vertex position with $\sim$20 μm accuracy. The two-level CMS trigger system selects events of interest for permanent storage. The first trigger level (L1), composed of custom hardware processors, uses information from the calorimeter and muon detectors to select events in less than 1 μs. The high-level trigger (HLT) software algorithms, executed on a farm of commercial processors, further reduce the event rate using information from all detector subsystems. A more detailed description of the CMS detector can be found elsewhere [8].

III. DATA SAMPLE AND EVENT RECONSTRUCTION

A. Event selection

The data sample used in this analysis was recorded by the CMS detector in pp collisions at a center-of-mass energy of 7 TeV. The sample corresponds to a total integrated luminosity of 3.1 ± 0.3 pb^{-1} [9]. The maximum instantaneous luminosity was 10^{31} cm^{-2} s^{-1}, and event pileup was negligible. Data are included in the analysis if the silicon tracker, the muon detectors, and the trigger were performing well, and the luminosity measurement is available.

The trigger requires the detection of two muons at the hardware level, without any further selection at the HLT. The coincidence of two muon signals without an explicit p_{T} requirement is sufficient to allow the dimuon trigger without prescaling. All three muon systems—DT, CSC, and resistive plate chambers—take part in the trigger decision.

Anomalous events arising from beam-gas interactions or beam scraping in the beam transport system near the interaction point, which produce a large number of hits in the pixel detector, are removed with offline software filters [10]. A good primary vertex is also required, as defined in Ref. [10].

B. Monte Carlo simulation

Upsilon events are simulated using PYTHIA 6.412 [6], which generates events based on the leading-order color-singlet and octet mechanisms, with nonrelativistic QCD matrix elements tuned by comparing calculations with the CDF data [11] and applying the normalization and wave-functions as recommended in Ref. [12]. The simulation includes the generation of χ_b states. Final-state radiation (FSR) is implemented using PHOTOS [13,14]. The response of the CMS detector is simulated with a GEANT4-based [15] Monte Carlo (MC) program. Simulated events are processed with the same reconstruction algorithms as used for data.

C. Offline muon reconstruction

In this analysis, a muon candidate is defined as a charged track reconstructed in the silicon tracker and associated with a compatible signal in the muon detectors. Tracks are reconstructed using a Kalman filter technique which starts from hits in the pixel system and extrapolates outward to the silicon strip tracker. Further details may be found in Ref. [16].

Quality criteria are applied to tracks to reject muons from kaon and pion decays. Tracks are required to have at least 12 hits in the silicon tracker, at least one of which must be in the pixel detector, and a track-fit χ^2 per degree of freedom smaller than 5. In addition tracks are required to emanate from a cylinder of radius 2 mm and length 50 cm centered on the pp interaction region and parallel to the beam line. Muon candidates are required to satisfy:

$$\begin{aligned} &p_{\mathrm{T}}^{\mu} > 3.5\ \mathrm{GeV}/c \quad \text{if } |\eta^{\mu}| < 1.6, \quad \text{or} \\ &p_{\mathrm{T}}^{\mu} > 2.5\ \mathrm{GeV}/c \quad \text{if } 1.6 < |\eta^{\mu}| < 2.4. \end{aligned} \tag{1}$$

These kinematic criteria are chosen to ensure that the trigger and muon reconstruction efficiencies are high and not rapidly changing within the acceptance window of the analysis.

The momentum measurement of charged tracks in the CMS detector is affected by systematic uncertainties caused by imperfect knowledge of the magnetic field, the amount of material, and subdetector misalignments, as well as by biases in the algorithms which fit the track trajectory. A mismeasurement of track momenta results in a shift and broadening of the reconstructed peaks of dimuon resonances. An improved understanding of the CMS magnetic field, detector alignment, and material budget is obtained from cosmic-ray muon and LHC collision data [7,17,18]. Residual effects are determined by studying the dependence of the reconstructed J/ψ dimuon invariant-mass distribution on the muon kinematics [19]. The transverse momentum corrected for the residual scale distortion is parametrized as $p_{\mathrm{T}} = (1 + a_1 + a_2\eta^2) \times p'_{\mathrm{T}}$, where p'_{T} is the measured muon transverse momentum, $a_1 = (3.8 \pm 1.9) \times 10^{-4}$, and $a_2 = (3.0 \pm 0.7) \times 10^{-4}$. Coefficients for terms linear in η and quadratic in p'_{T} and $p'_{\mathrm{T}} \cdot \eta$ are consistent with zero and are not included.

D. Υ event selection

To identify events containing an Υ decay, muon candidates with opposite charges are paired, and the invariant mass of the muon pair is required to be between 8 and 14 GeV/c^2. The longitudinal separation between the two muons at their points of closest approach to the beam axis

is required to be less than 2 cm. The two muon helices are fit with a common vertex constraint, and events are retained if the fit χ^2 probability is larger than 0.1%. The dimuon candidate is required to have passed the trigger selection. If multiple dimuon candidates are found in the same event, the candidate with the best vertex quality is retained; the fraction of signal candidates rejected by this requirement is about 0.2%. Finally, the rapidity, y, of the Υ candidates is required to satisfy $|y| < 2$ because the acceptance diminishes rapidly at larger rapidity. The rapidity is defined as

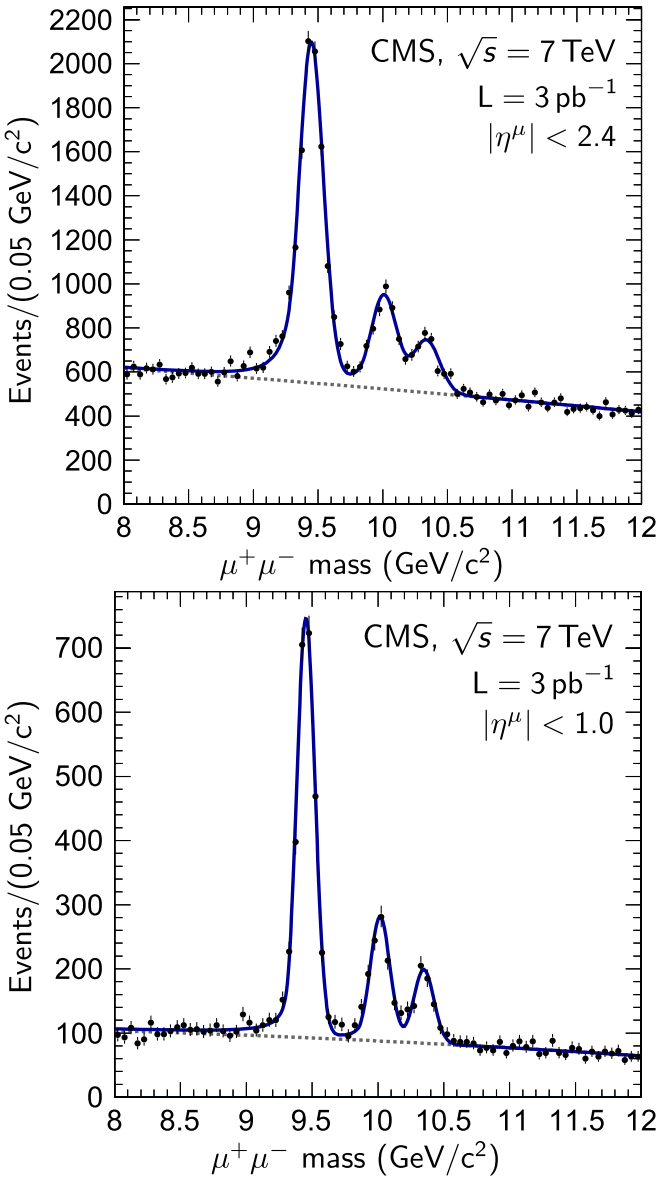


FIG. 1 (color online). The dimuon invariant-mass distribution in the vicinity of the $\Upsilon(nS)$ resonances for the full rapidity covered by the analysis (top) and for the subset of events where the pseudorapidity of each muon satisfies $|\eta^\mu| < 1$ (bottom). The solid line shows the result of a fit to the invariant-mass distribution before accounting for acceptance and efficiency, with the dashed line denoting the background component. Details of the fit are described in Sec. VI.

$y = \frac{1}{2}\ln(\frac{E+p_\parallel}{E-p_\parallel})$, where E is the energy and $p_\parallel$ the momentum parallel to the beam axis of the muon pair.

The dimuon invariant-mass spectrum in the $\Upsilon(nS)$ region for the dimuon transverse-momentum interval $p_T < 30$ GeV/c is shown in Fig. 1 for the pseudorapidity intervals $|\eta^\mu| < 2.4$ (top) and $|\eta^\mu| < 1.0$ (bottom). The $\Upsilon(1S)$ mass resolution is determined from the fit function described in Sec. VI. We obtain a mass resolution of 96 ± 2 MeV/c^2 when muons from the entire pseudorapidity range are included and 69 ± 2 MeV/c^2 when both muons satisfy $|\eta^\mu| < 1$. The observed resolutions are in good agreement with the predictions from MC simulation.

IV. ACCEPTANCE

The $\Upsilon \to \mu^+\mu^-$ acceptance of the CMS detector is defined as the product of two terms. The first is the fraction of upsilons of given p_T and y where each of the two muons satisfies Eq. (1). The second is the probability that when there are only two muons in the event both can be reconstructed in the tracker without requiring the quality criteria. Both terms are evaluated by simulation and parametrized as a function of the p_T and rapidity of the Υ.

The acceptance is calculated from the ratio

$$\mathcal{A}^\Upsilon(p_T, y) = \frac{N^\Upsilon_{\rm rec}(p_T, y)}{N^\Upsilon_{\rm gen}(p_T, y)}, \tag{2}$$

where $N^\Upsilon_{\rm gen}(p_T, y)$ is the number of upsilons generated in a (p_T, y) bin, while $N^\Upsilon_{\rm rec}(p_T, y)$ is the number reconstructed in the same (p_T, y) region but now using the reconstructed, rather than generated, variables. In addition, the numerator requires that the two muons reconstructed in the silicon tracker satisfy Eq. (1).

The acceptance is evaluated with a signal MC sample in which the Υ decay to two muons is generated with the EVTGEN [20] package including the effects of final-state radiation. There are no particles in the event besides the Υ, its daughter muons, and final-state radiation. The upsilons are generated uniformly in p_T and rapidity. This sample is then fully simulated and reconstructed with the CMS detector simulation software to assess the effects of multiple scattering and finite resolution of the detector. Systematic uncertainties arising from the dependence of the measurement of the cross section on the MC description of the p_T spectrum and resolution are evaluated in Sec. VII. The acceptance is calculated for two-dimensional (2-D) bins of size (1 GeV/c, 0.1) in the reconstructed (p_T, y) of the Υ, and it is used in candidate-by-candidate yield corrections.

The 2-D acceptance map for unpolarized $\Upsilon(1S)$ is shown in the top plot of Fig. 2. The acceptance varies with dimuon mass. This is shown in the bottom plot of Fig. 2, which displays the acceptance integrated over the rapidity range as a function of p_T for each upsilon resonance. The transverse-momentum threshold for muon detection, especially in the forward region, is small compared

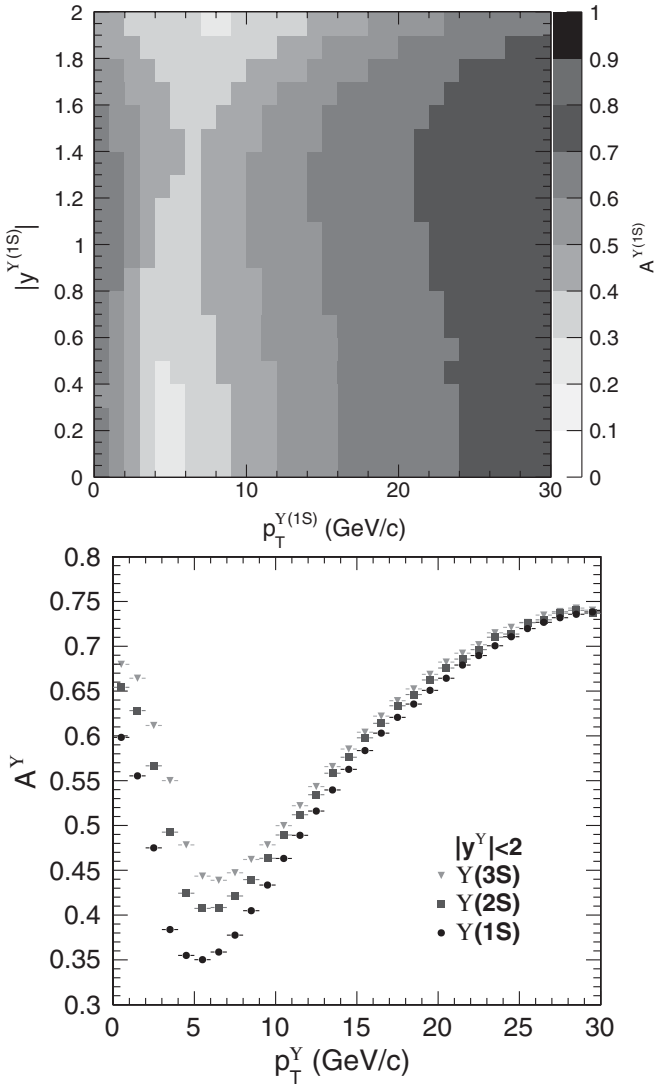


FIG. 2. (Top) Unpolarized $\Upsilon(1S)$ acceptance as a function of p_T and y; (bottom) the unpolarized $\Upsilon(1S)$, $\Upsilon(2S)$, and $\Upsilon(3S)$ acceptances integrated over rapidity as a function of p_T.

to the upsilon mass. Therefore, when the Υ decays at rest, both muons are likely to reach the muon detector. When the Υ has a modest boost, the probability is greater that one muon will be below the muon detection threshold and the acceptance decreases until the Υ transverse momentum reaches about 5 GeV/c, after which the acceptance rises slowly. The production polarization of the Υ strongly influences the muon angular distributions and is expected to change as a function of p_T. In order to account for this, the acceptance is calculated for five extreme polarization scenarios [21]: unpolarized and polarized longitudinally and transversely with respect to a polarization axis defined in two different reference frames. The first is the helicity frame (HX), where the polarization axis is given by the flight direction of the Υ in the center-of-mass system of the colliding beams. The second is the Collins-Soper (CS) frame [22], where the polarization axis is given as the bisection of the incoming proton directions in the Υ rest frame.

V. EFFICIENCY

We factor the total muon efficiency into three conditional terms,

$$\varepsilon(\text{total}) = \varepsilon(\text{trig}|\text{id}) \cdot \varepsilon(\text{id}|\text{track}) \cdot \varepsilon(\text{track}|\text{accepted}) \equiv \varepsilon_{\text{trig}} \cdot \varepsilon_{\text{id}} \cdot \varepsilon_{\text{track}}. \quad (3)$$

The tracking efficiency, $\varepsilon_{\text{track}}$, combines the efficiency that the accepted track of a muon from the $\Upsilon(nS)$ decay is reconstructed in the presence of additional particles in the silicon tracker, as determined with a track-embedding technique [23], and the efficiency for the track to satisfy quality criteria. The muon identification efficiency, ε_{id}, is the probability that the track in the silicon tracker is identified as a muon. The efficiency that an identified muon satisfies the trigger is denoted by $\varepsilon_{\text{trig}}$.

The tag-and-probe (T&P) technique [23] is a data-based method used in this analysis to determine the track quality, muon identification, and muon trigger efficiencies. It utilizes dimuons from J/ψ decays to provide a sample of probe objects. A well-identified muon, the tag, is combined with a second object in the event, the probe, and the invariant mass is computed. The tag-probe pairs are divided into two samples, depending on whether the probe satisfies or not the criteria for the efficiency being evaluated. The two tag-probe mass distributions contain a J/ψ peak. The integral of the peak is the number of probes that satisfy or fail to satisfy the imposed criteria. The efficiency parameter is extracted from a simultaneous unbinned maximum-likelihood fit to both mass distributions.

The J/ψ resonance is utilized for T&P efficiency measurements as it provides a large-yield and statistically-independent dimuon sample [24]. To avoid trigger bias, events containing a tag-probe pair have been collected with triggers that do not impose requirements on the probe from the detector subsystem related to the efficiency measurement. For the track-quality efficiency measurement, the trigger requires two muons at L1 in the muon system without using the silicon tracker. For the muon identification and trigger efficiencies, the trigger requires a muon at the HLT, that is matched to the tag, paired with a silicon track of opposite sign and the invariant mass of the pair is required to be in the vicinity of the J/ψ mass.

The component of the tracking efficiency measured with the track-embedding technique is well described by a constant value of $(99.64 \pm 0.05)\%$. The efficiency of the track-quality criteria measured by the T&P method is likewise nearly uniform and has an average value of $(98.66 \pm 0.05)\%$. Tracks satisfying the quality criteria are the probes for the muon identification study. The resulting single-muon identification efficiencies as a function of p_T^{μ} for six $|\eta^{\mu}|$ regions are shown in Fig. 3

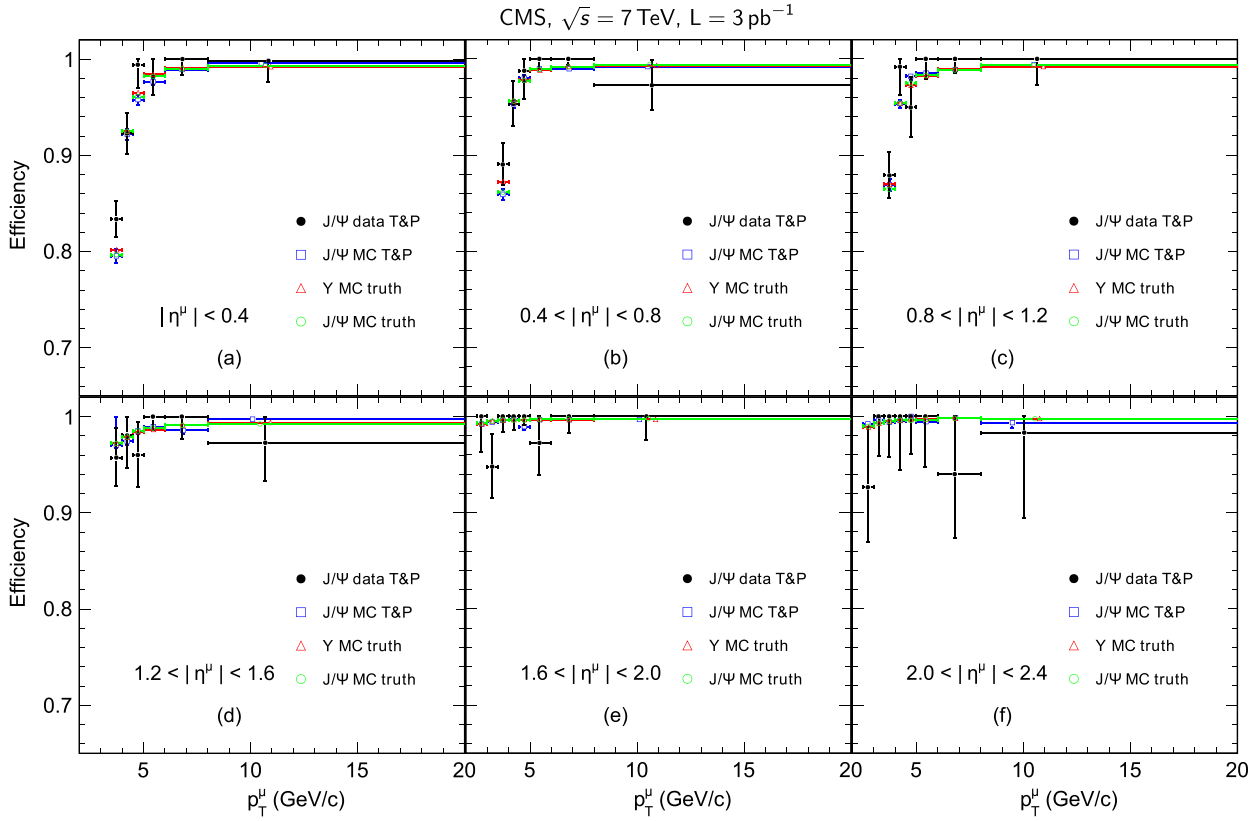


FIG. 3 (color online). Single-muon identification efficiencies as a function of p_T^μ for six $|\eta^\mu|$ regions, measured from data using J/ψ T&P (closed circles). The efficiencies determined with Υ MC truth (triangles), J/ψ MC truth (open circles), and J/ψ MC T&P (squares), used in the evaluation of systematic uncertainties, are also shown.

and Table I. The probes that satisfy the muon identification criteria are in turn the probes for the study of the trigger efficiency. The resulting trigger efficiencies for the same p_T^μ and $|\eta^\mu|$ regions are shown in Fig. 4 and Table II.

Figs. 3 and 4 also show single-muon identification and trigger efficiencies, respectively, determined from a high-statistics MC simulation. The single-muon efficiencies determined with the T&P technique in the data are found to be consistent, over most of the kinematic range of interest, with the efficiencies obtained from the Υ MC simulation utilizing the generator-level particle information ("MC truth"). Two exceptions are the single-muon trigger efficiency for the intervals $|\eta^\mu| < 0.4$ and $0.8 < |\eta^\mu| < 1.2$, where the efficiency is lower in data than in the MC simulation. Both correspond to cases where the MC simulation is known to not fully reproduce the detector properties or performance: gaps in the DT coverage ($|\eta^\mu| < 0.4$) and suboptimal timing synchronization

TABLE I. Single-muon identification efficiencies, in percent, measured from J/ψ data with T&P. The statistical uncertainties in the least significant digits are given in parentheses; uncertainties less than 0.05 are denoted by 0. For asymmetric uncertainties the positive uncertainty is reported first.

p_T^μ	$\lvert\eta^\mu\rvert$					
(GeV/c)	0.0–0.4	0.4–0.8	0.8–1.2	1.2–1.6	1.6–2.0	2.0–2.4
2.5–3.0					100(0, 4)	94(6)
3.0–3.5					95(3)	100(0, 4)
3.5–4.0	83(2)	89(2)	88(2)	96(3)	100(0, 2)	100(0, 4)
4.0–4.5	92(2)	95(2)	99(1, 3)	98(2, 3)	100(0, 2)	100(0, 6)
4.5–5.0	99(1, 2)	99(1, 3)	95(3)	96(3)	100(0, 2)	100(0, 4)
5.0–6.0	98(2)	100(0, 1)	100(0, 2)	100(0, 1)	97(3)	100(0, 5)
6.0–8.0	100(0, 2)	100(0, 1)	100(0, 1)	100(0, 2)	100(0, 2)	94(6, 7)
8.0–50.0	100(0, 2)	97(3)	100(0, 3)	97(3, 4)	100(0, 3)	98(2, 9)

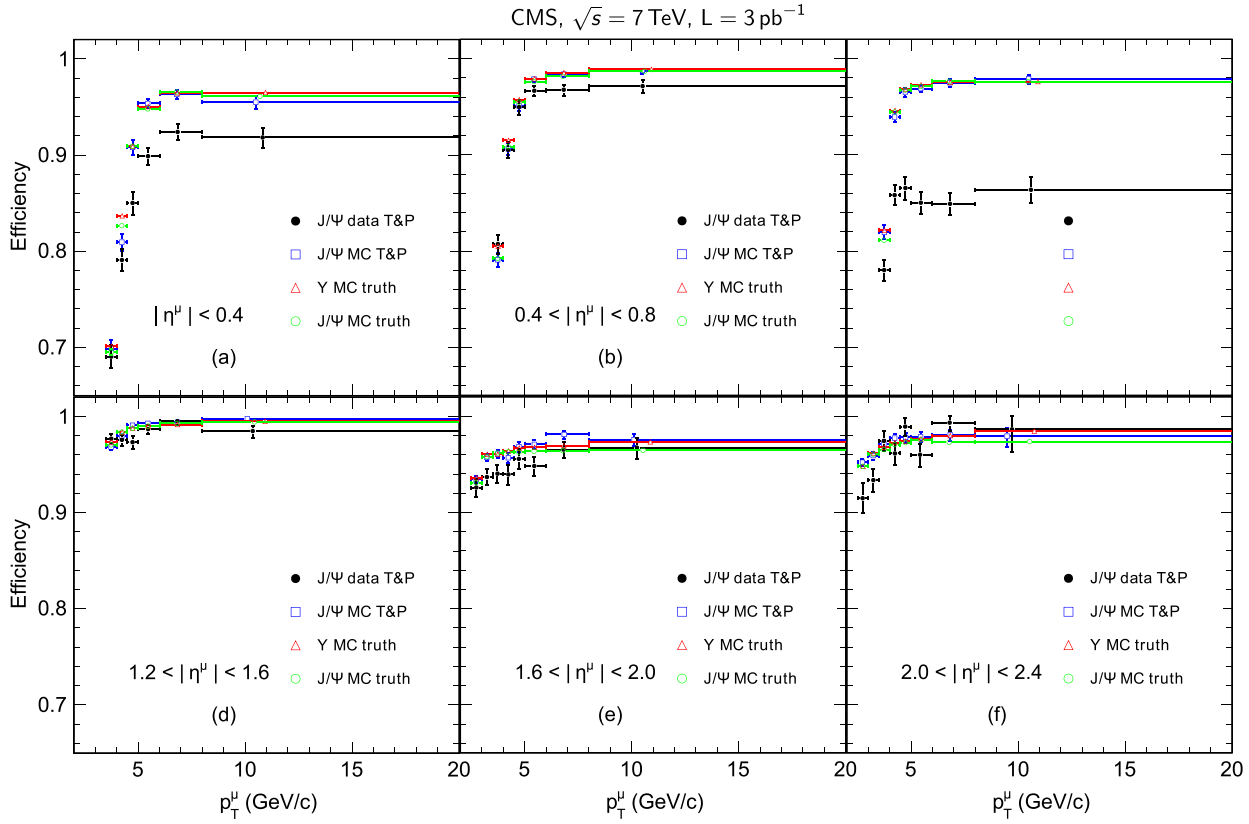


FIG. 4 (color online). Single-muon trigger efficiencies as a function of p_T^μ for six $|\eta^\mu|$ regions, measured from data using J/ψ T&P (closed circles). The efficiencies determined with Υ MC truth (triangles), J/ψ MC truth (open circles), and J/ψ MC T&P (squares), used in the evaluation of systematic uncertainties, are also shown.

between the overlapping CSC and DT subsystems ($0.8 < |\eta^\mu| < 1.2$). For all cases the data-determined efficiencies are used to obtain the central results.

The Υ efficiency is estimated from the product of single-muon efficiencies. Differences between the single and dimuon efficiencies determined from MC truth and those measured with the T&P technique can arise from the kinematic distributions of the probes and from bin averaging.

TABLE II. Single-muon trigger efficiencies, in percent, measured from J/ψ data with T&P. The statistical uncertainties in the least significant digits are given in parentheses; uncertainties less than 0.05 are denoted by 0. For asymmetric uncertainties the positive uncertainty is reported first.

p_T^μ	$\lvert\eta^\mu\rvert$					
(GeV/c)	0.0–0.4	0.4–0.8	0.8–1.2	1.2–1.6	1.6–2.0	2.0–2.4
2.5–3.0					93(1)	92(2)
3.0–3.5					94(1)	93(1)
3.5–4.0	69(1)	81(1)	78(1)	98(1)	94(1)	97(1)
4.0–4.5	79(1)	91(1)	86(1)	98(1)	92(1)	96(1)
4.5–5.0	85(1)	95(1)	87(1)	97(1)	96(1)	99(1)
5.0–6.0	90(1)	97(1)	85(1)	99(0, 1)	95(1)	96(1)
6.0–8.0	92(1)	97(1)	85(1)	100(0)	97(1)	99(1)
8.0–50.0	92(1)	97(1)	86(1)	99(1)	97(1)	99(2)

This is evaluated by comparing the single-muon and dimuon efficiencies as determined using the T&P method in $J/\psi \to \mu^+\mu^-$ MC events to the efficiencies obtained in the same events utilizing generator-level particle information. In addition, effects arising from differences in the kinematic distributions between the Υ and J/ψ decay muons are investigated by comparing the efficiencies determined from $\Upsilon \to \mu^+\mu^-$ MC events to those from $J/\psi \to \mu^+\mu^-$ MC events. In all cases the differences in the efficiency values are not significant, and are used only as an estimate of the associated systematic uncertainties.

The efficiency of the vertex χ^2 probability cut is determined using the high-statistics J/ψ data sample, to which the Υ selection criteria are applied. The efficiency is extracted from a simultaneous fit to the dimuon mass distribution of the passing and failing candidates. It is found to be $(99.2 \pm 0.1)\%$. A possible difference between the efficiency of the vertex χ^2 probability cut for the J/ψ and Υ is evaluated by applying the same technique to large MC signal samples of each resonance. No significant difference in the efficiencies is found. The efficiency of the remaining selection criteria listed in Sec. III is studied in data and MC simulation and is found to be consistent with unity.

VI. MEASUREMENT OF THE CROSS SECTIONS

The $\Upsilon(nS)$ differential cross section is determined from the acceptance and efficiency-corrected signal yield, $N^{\text{corrected}}_{\Upsilon(nS)}$, using the equation

$$\frac{d^2\sigma(pp \to \Upsilon(nS)X)}{dp_{\mathrm{T}}dy} \cdot \mathcal{B}(\Upsilon(nS) \to \mu^+\mu^-) = \frac{N^{\text{corrected}}_{\Upsilon(nS)}(\mathcal{A}, \varepsilon)}{\mathcal{L} \cdot \Delta p_{\mathrm{T}} \cdot \Delta y}, \quad (4)$$

where $\mathcal{L}$ is the integrated luminosity of the dataset and Δp_{T} and Δy are the bin widths.

The $\Upsilon(1S)$, $\Upsilon(2S)$, and $\Upsilon(3S)$ yields are extracted via an extended unbinned maximum-likelihood fit to the dimuon invariant-mass spectrum. The measured mass-lineshape of each Υ state is parametrized by a "crystal ball" (CB) function [25]; this is a Gaussian resolution function with the low side tail replaced with a power law describing FSR. The resolution, given by the Gaussian standard deviation, is a free parameter in the fit but is constrained to scale with the ratios of the resonance masses. The FSR tail is fixed to the MC shape. Since the three resonances overlap in the measured dimuon mass, we fit the three $\Upsilon(nS)$ states simultaneously. Therefore, the probability distribution function (PDF) describing the signal consists of three CB

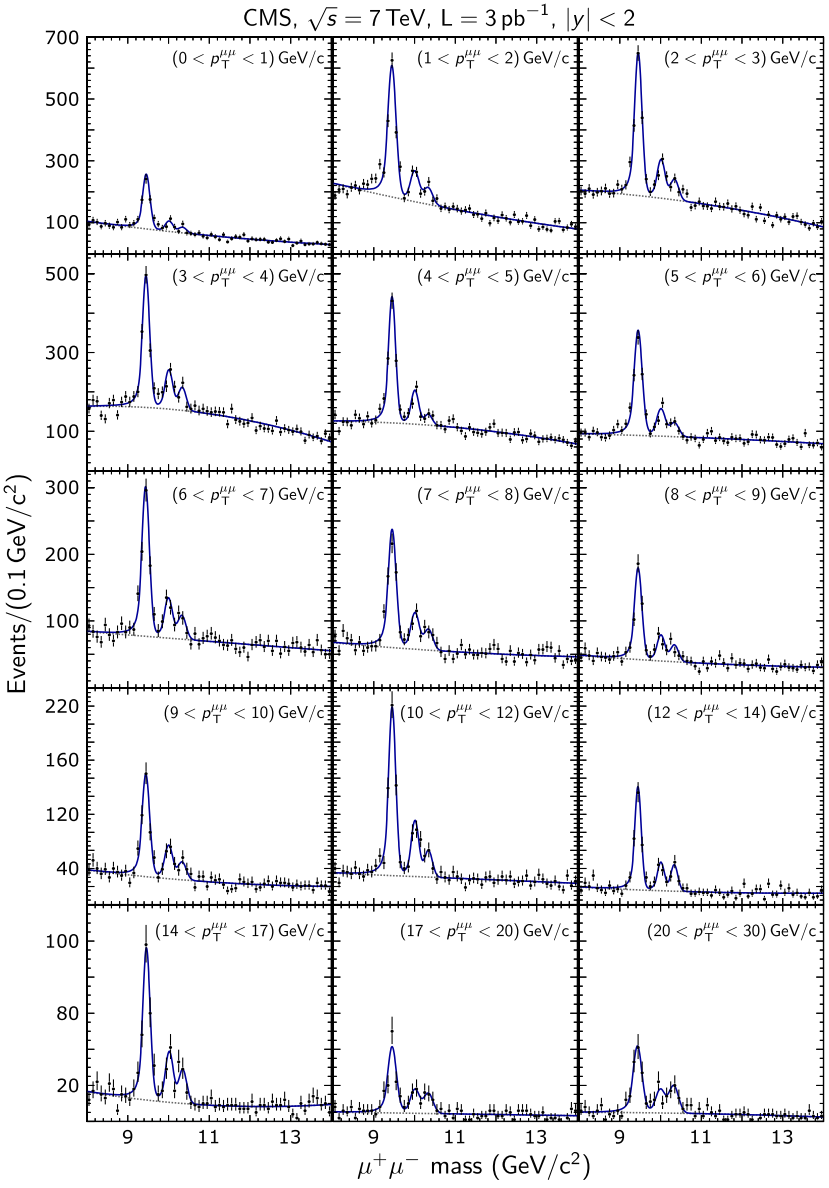


FIG. 5 (color online). Fit to the dimuon invariant-mass distribution in the specified p_{T} regions for $|y| < 2$, before accounting for acceptance and efficiency. The solid line shows the result of the fit described in the text, with the dashed line representing the background component.

functions. The mass of the $\Upsilon(1S)$ is a free parameter in the fit, to accommodate a possible bias in the momentum scale calibration. The number of free parameters is reduced by fixing the $\Upsilon(2S)$ and $\Upsilon(3S)$ mass differences, relative to the $\Upsilon(1S)$, to their world average values [26]; an additional mass-scale parameter multiplying the mass differences is found to be consistent with unity. A second-order polynomial is chosen to describe the background in the 8–14 GeV/c^2 mass-fit range.

The fit to the dimuon invariant-mass spectrum, before accounting for acceptance and efficiencies, is shown in Fig. 1 for the Υ transverse-momentum interval $p_T < 30$ GeV/c, and for the 15 p_T intervals used for the $\Upsilon(1S)$ differential cross-section measurement in Fig. 5. The observed $\Upsilon(nS)$ signal yields are reported in Table III. The width of the p_T intervals chosen for each resonance reflects the corresponding available signal statistics. In all cases the quoted uncertainty is statistical. As shown in Table III, for each resonance the sum of the yields in each p_T interval is consistent with the yield determined from a fit to the entire p_T range. Given the significant η and p_T dependencies of the efficiencies and acceptances of the muons from $\Upsilon(nS)$ decays, we correct for them on a candidate-by-candidate basis before performing the mass fit to obtain $N^{\text{corrected}}_{\Upsilon(nS)}$ in Eq. (4). Specifically: an Υ candidate reconstructed with p_T and y from muons with $p_T^{\mu_{1,2}}$ and $\eta^{\mu_{1,2}}$ is corrected with a weight

TABLE III. The uncorrected Υ signal yield, fit quality (normalized χ^2, obtained by comparing the fit PDF and the binned data; the number of degrees of freedom is 112), and average weight $\langle w \rangle$ in p_T intervals for $|y| < 2$. The mean of the p_T distribution in each interval is also given.

	p_T range	(GeV/c) mean	fit χ^2	signal yield	$\langle w \rangle^{-1}$
$\Upsilon(1S)$	0–1	0.7	1.1	427 ± 34	0.44
	1–2	1.5	1.7	1153 ± 54	0.41
	2–3	2.5	1.1	1154 ± 53	0.36
	3–4	3.5	1.3	806 ± 46	0.30
	4–5	4.5	1.0	769 ± 43	0.28
	5–6	5.5	1.1	716 ± 40	0.28
	6–7	6.5	1.2	578 ± 37	0.28
	7–8	7.5	1.3	477 ± 33	0.30
	8–9	8.5	1.1	344 ± 26	0.34
	9–10	9.5	1.1	286 ± 24	0.37
	10–12	10.9	1.1	449 ± 27	0.41
	12–14	12.9	1.3	246 ± 19	0.45
	14–17	15.4	1.2	208 ± 18	0.50
	17–20	18.3	0.8	105 ± 13	0.54
	20–30	23.3	0.8	109 ± 13	0.60
	sum			7825 ± 133	
	combined fit			7807 ± 133	
$\Upsilon(2S)$	0–2	1.3	1.7	368 ± 41	0.47
	2–4	2.9	1.3	591 ± 50	0.40
	4–6	4.9	0.9	416 ± 40	0.32
	6–9	7.3	1.1	424 ± 38	0.33
	9–12	10.3	1.1	257 ± 25	0.41
	12–16	13.6	1.3	121 ± 16	0.46
	16–20	17.7	1.0	63 ± 11	0.55
	20–30	22.5	0.8	39 ± 9	0.60
	sum			2279 ± 91	
	combined fit			2270 ± 91	
$\Upsilon(3S)$	0–3	1.8	1.5	397 ± 51	0.47
	3–6	4.3	1.0	326 ± 47	0.37
	6–9	7.3	1.1	264 ± 36	0.35
	9–14	11.0	1.2	207 ± 25	0.43
	14–20	16.3	1.2	83 ± 14	0.52
	20–30	23.4	0.8	49 ± 10	0.61
	sum			1324 ± 84	
	combined fit			1318 ± 84	

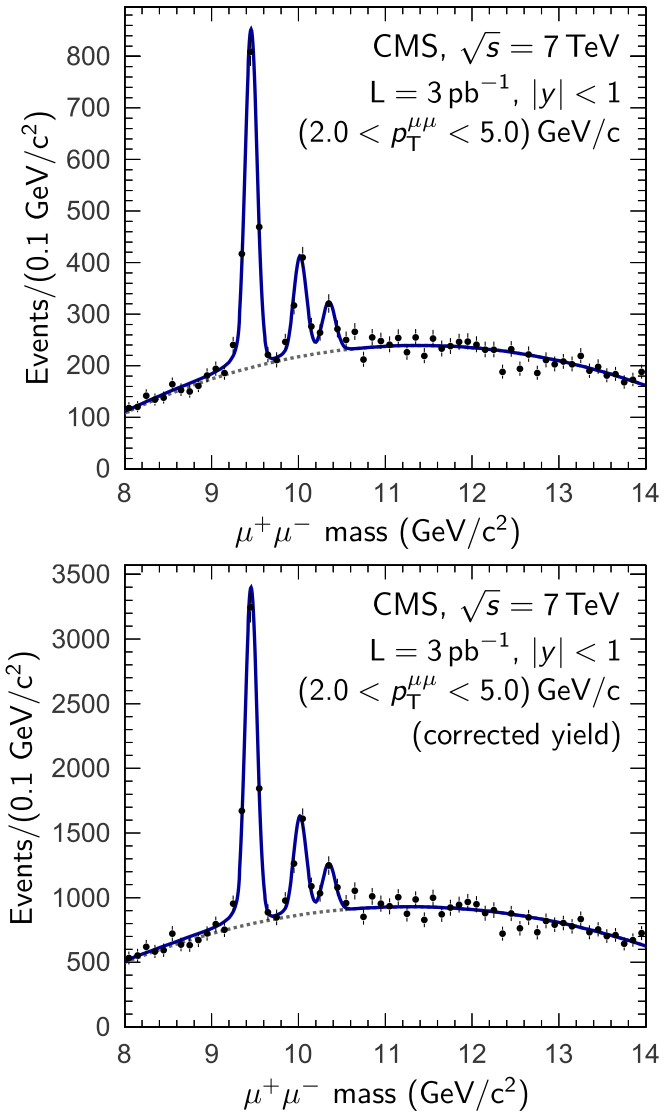


FIG. 6 (color online). (Top) Fit to the dimuon invariant-mass distribution in the range $2 < p_T < 5$ GeV/c for $|y| < 1$. (bottom) Fit to the $\Upsilon(1S)$-acceptance and efficiency weighted dimuon distribution in the range $2 < p_T < 5$ GeV/c for $|y| < 1$.

$$w \equiv w_{\rm acc} \cdot w_{\rm track} \cdot w_{\rm id} \cdot w_{\rm trig} \cdot w_{\rm misc}, \quad (5)$$

where the factors are: (i) acceptance, $w_{\rm acc} = 1/\mathcal{A}^{\Upsilon}(p_{\rm T}, y)$; (ii) tracking, $w_{\rm track} = 1/[\varepsilon_{\rm track}(p_{\rm T}^{\mu_1}, \eta^{\mu_1}) \cdot \varepsilon_{\rm track}(p_{\rm T}^{\mu_2}, \eta^{\mu_2})]$; (iii) identification, $w_{\rm id} = 1/[\varepsilon_{\rm id}(p_{\rm T}^{\mu_1}, \eta^{\mu_1}) \cdot \varepsilon_{\rm id}(p_{\rm T}^{\mu_2}, \eta^{\mu_2})]$; (iv) trigger, $w_{\rm trig} = 1/[\varepsilon_{\rm trig}(p_{\rm T}^{\mu_1}, \eta^{\mu_1}) \cdot \varepsilon_{\rm trig}(p_{\rm T}^{\mu_2}, \eta^{\mu_2})]$; and (v) additional selection criteria, $w_{\rm misc}$, including the efficiency of the vertex selection criteria. The acceptance depends on the resonance mass; the $\Upsilon(3S)$ gives rise to higher-momenta muons which results in a roughly 10% larger acceptance for the $\Upsilon(3S)$ than for the $\Upsilon(1S)$. Consequently, the corrected yield for each of the $\Upsilon(nS)$ resonances is obtained from a fit in which the corresponding $\Upsilon(nS)$ acceptance is employed. Figure 6 shows the fit to an example mass distribution before (top plot) and after (bottom plot) event weighting. As can be seen, the weighting procedure scales the mass distribution without introducing large distortions to the lineshape of either the signal or background distributions.

We determine the $\Upsilon(nS)$ differential cross section separately for each polarization scenario. The results are summarized in Table IV. We also divide the data into two ranges of rapidity, $|y| < 1$ and $1 < |y| < 2$, and repeat the

TABLE IV. The product of the $\Upsilon(nS)$ production cross sections, σ, and the dimuon branching fraction, $\mathcal{B}$, measured in $p_{\rm T}$ bins for $|y| < 2$, with the assumption of unpolarized production. The statistical uncertainty (stat.), the sum of the systematic uncertainties in quadrature ($\Sigma_{\rm syst.}$), and the total uncertainty ($\Delta\sigma$; including stat., $\sum_{\rm syst.}$, and luminosity terms) are quoted as relative uncertainties in percent. Values in parentheses denote the negative part of the asymmetric uncertainty. The fractional change in percent of the cross section is shown for four polarization scenarios: fully-longitudinal (L) and fully-transverse (T) in the helicity (HX) and Collins-Soper (CS) frames.

$p_{\rm T}$ (GeV/c)	$\sigma \cdot \mathcal{B}$ (nb)	stat. (%)	$\sum_{\rm syst.}$ (%)	$\Delta\sigma$ (%)	HX-T (%)	HX-L (%)	CS-T (%)	CS-L (%)
		$\Upsilon(1S)$				$\lvert y\rvert < 2$		
0–30	7.37	1.8	8(6)	14(13)	+16	−22	+13	−16
0–1	0.30	8	10(7)	17(15)	+16	−22	+17	−23
1–2	0.90	5	9(6)	15(14)	+16	−20	+19	−24
2–3	1.04	5	8(6)	14(13)	+15	−20	+19	−24
3–4	0.88	6	9(7)	15(14)	+18	−23	+18	−23
4–5	0.90	6	8(6)	15(14)	+18	−23	+16	−21
5–6	0.82	6	8(6)	15(14)	+17	−23	+13	−19
6–7	0.64	7	8(5)	15(14)	+17	−22	+11	−16
7–8	0.51	7	8(6)	15(14)	+16	−22	+7	−10
8–9	0.33	8	8(6)	16(14)	+16	−22	+4	−5
9–10	0.25	8	9(6)	16(15)	+15	−21	+2	−1
10–12	0.36	6	8(5)	15(14)	+15	−21	−1	+3
12–14	0.18	8	9(5)	16(14)	+15	−20	−3	+7
14–17	0.14	9	10(6)	17(15)	+14	−19	−4	+9
17–20	0.06	12	10(6)	19(17)	+13	−18	−4	+10
20–30	0.06	12	10(6)	19(17)	+12	−17	−4	+10
		$\Upsilon(2S)$				$\lvert y\rvert < 2$		
0–30	1.90	4.2	9(6)	15(13)	+14	−19	+12	−15
0–2	0.25	12	11(9)	20(19)	+14	−19	+17	−22
2–4	0.48	8	12(10)	18(17)	+12	−17	+18	−23
4–6	0.41	10	10(8)	18(17)	+16	−22	+15	−20
6–9	0.41	9	10(7)	17(16)	+15	−21	+9	−13
9–12	0.21	10	9(6)	17(16)	+14	−20	+1	−0
12–16	0.09	13	10(7)	20(19)	+14	−19	−2	+6
16–20	0.04	18	11(8)	24(23)	+12	−18	−4	+9
20–30	0.02	23	20(18)	32(32)	+12	−17	−5	+11
		$\Upsilon(3S)$				$\lvert y\rvert < 2$		
0–30	1.02	6.7	11(8)	17(15)	+14	−19	+10	−13
0–3	0.26	14	10(8)	21(19)	+13	−18	+16	−22
3–6	0.29	14	18(17)	26(25)	+13	−18	+16	−21
6–9	0.24	14	11(8)	21(19)	+15	−20	+10	−13
9–14	0.16	12	10(8)	19(18)	+15	−20	−1	+2
14–20	0.05	17	11(8)	23(22)	+13	−18	−4	+9
20–30	0.03	20	12(9)	26(25)	+11	−16	−4	+9

TABLE V. The product of the $\Upsilon(nS)$ production cross sections, σ, and the dimuon branching fraction, $\mathcal{B}$, measured in p_T bins for $|y| < 1$ and $1 < |y| < 2$, with the assumption of unpolarized production. The statistical uncertainty (stat.), the sum of the systematic uncertainties in quadrature ($\Sigma_{\text{syst.}}$), and the total uncertainty ($\Delta\sigma$; including stat., $\sum_{\text{syst.}}$, and luminosity terms) are quoted as relative uncertainties in percent. Values in parentheses denote the negative part of the asymmetric uncertainty. The fractional change in percent of the cross section is shown for four polarization scenarios: fully-longitudinal (L) and fully-transverse (T) in the helicity (HX) and Collins-Soper (CS) frames.

p_T (GeV/c)	$\sigma \cdot \mathcal{B}$ (nb)	stat. (%)	$\sum_{\text{syst.}}$ (%)	$\Delta\sigma$ (%)	HX-T (%)	HX-L (%)	CS-T (%)	CS-L (%)
		$\Upsilon(1S)$				$\|y\| < 1$		
0–30	4.03	1.3	8(6)	14(12)	+16	−22	+13	−16
0–2	0.70	5	9(7)	15(14)	+14	−19	+18	−24
2–5	1.54	4	10(9)	15(15)	+14	−20	+18	−23
5–8	1.02	5	7(6)	14(13)	+18	−23	+8	−12
8–11	0.44	6	7(5)	15(14)	+18	−23	−1	+2
11–15	0.23	7	8(5)	15(14)	+18	−23	−4	+10
15–30	0.11	9	8(6)	16(15)	+15	−20	−5	+12
		$\Upsilon(2S)$				$\|y\| < 1$		
0–30	1.03	2.9	9(6)	15(13)	+14	−19	+12	−15
0–3	0.29	10	17(16)	22(21)	+10	−14	+17	−22
3–7	0.41	10	16(15)	21(21)	+13	−18	+14	−19
7–11	0.22	11	9(7)	18(17)	+17	−22	+1	−2
11–15	0.06	16	9(6)	21(20)	+17	−22	−4	+8
15–30	0.04	17	9(7)	22(21)	+14	−20	−5	+11
		$\Upsilon(3S)$				$\|y\| < 1$		
0–30	0.59	4.8	11(8)	16(15)	+14	−19	+10	−13
0–7	0.38	11	25(24)	30(29)	+11	−16	+14	−19
7–12	0.15	15	10(8)	21(20)	+16	−22	+1	−1
12–30	0.07	14	10(8)	20(20)	+15	−21	−4	+10
		$\Upsilon(1S)$				$1 < \|y\| < 2$		
0–30	3.55	1.2	8(6)	14(12)	+16	−22	+13	−16
0–2	0.55	7	11(9)	17(16)	+18	−24	+18	−23
2–5	1.39	4	9(7)	15(14)	+20	−25	+18	−23
5–8	0.97	5	9(5)	15(13)	+16	−22	+14	−18
8–11	0.37	7	10(6)	16(14)	+13	−19	+6	−8
11–15	0.18	8	10(6)	17(15)	+11	−17	0	+1
15–30	0.10	17(15)	11(6)	18(16)	+10	−16	−3	+6
		$\Upsilon(2S)$				$1 < \|y\| < 2$		
0–30	0.93	3.0	9(6)	15(13)	+14	−19	+12	−15
0–3	0.21	15	24(23)	30(29)	+17	−23	+17	−23
3–7	0.44	9	12(8)	18(17)	+17	−22	+17	−22
7–11	0.19	12	11(8)	20(18)	+13	−18	+9	−12
11–15	0.06	17	11(7)	23(21)	+11	−17	+1	0
15–30	0.03	21	13(9)	27(26)	+10	−16	−3	+7
		$\Upsilon(3S)$				$1 < \|y\| < 2$		
0–30	0.40	4.9	11(8)	16(15)	+14	−19	+10	−13
0–7	0.24	18	29(27)	36(35)	+16	−22	+17	−22
7–12	0.10	22	13(10)	28(27)	+13	−18	+10	−13
12–30	0.06	17	11(8)	23(22)	+10	−15	−2	+5

fits to obtain the $\Upsilon(nS)$ differential cross sections reported in Table V. The integrated cross section for each resonance is obtained from the corresponding sum of the differential cross sections. The results for the $\Upsilon(1S)$ p_T-integrated, rapidity-differential cross section are shown in Table VI.

VII. SYSTEMATIC UNCERTAINTIES

Systematic uncertainties are described in this section, together with the methods used in their determination. We give a representative value for each uncertainty in parentheses.

TABLE VI. The product of the $\Upsilon(1S)$ production cross section, σ, and the dimuon branching fraction, $\mathcal{B}$, measured in rapidity bins and integrated over the p_T range $p_T^\Upsilon < 30$ GeV/c, with the assumption of unpolarized production. The statistical uncertainty (stat.), the sum of the systematic uncertainties in quadrature ($\Sigma_{\text{syst.}}$), and the total uncertainty ($\Delta\sigma$; including stat., $\sum_{\text{syst.}}$, and luminosity terms) are quoted as relative uncertainties in percent. Values in parentheses denote the negative part of the asymmetric uncertainty. The fractional change in percent of the cross section is shown for four polarization scenarios: fully-longitudinal (L) and fully-transverse (T) in the helicity (HX) and Collins-Soper (CS) frames.

$\lvert y\rvert$	$\sigma \cdot \mathcal{B}$ (nb)	stat. (%) $\Upsilon(1S)$	$\sum_{\text{syst.}}$ (%)	$\Delta\sigma$ (%)	HX-T (%)	HX-L (%)	CS-T (%)	CS-L (%)
					$p_T < 30$ GeV/c			
0.0–2.0	7.61	1.8	8(6)	14(13)	+16	−22	+13	−16
0.0–0.4	1.62	3	8(6)	14(13)	+15	−19	+13	−17
0.4–0.8	1.52	4	9(8)	15(14)	+17	−22	+11	−15
0.8–1.2	1.77	4	9(7)	14(13)	+16	−22	+9	−12
1.2–1.6	1.47	4	9(7)	15(13)	+17	−23	+12	−16
1.6–2.0	1.23	4	11(7)	16(14)	+18	−23	+20	−24

We determine the cross section using acceptance maps corresponding to five different polarization scenarios, expected to represent extreme cases. The values of the cross section obtained vary by about 20%. The variations depend on p_T thus affecting the shapes of the p_T spectrum.

The statistical uncertainties on the acceptance and efficiencies—single-muon trigger and muon ID, quality criteria, tracking and vertex quality—give rise to systematic uncertainties for the cross-section measurement. We vary the dimuon event weights in the fit coherently by $\pm 1\sigma$(stat.). The muon identification and trigger efficiencies are varied coherently when estimating the associated systematic uncertainties (8%).

The selection criteria requiring the muons to be consistent with emanating from the same primary vertex are fully efficient. This has been confirmed in data and simulation. The selection of one candidate per event using the largest vertex probability also has an efficiency consistent with unity. We assign an uncertainty (0.2%) from the frequency of occurrence of signal candidates in the data that are rejected by the largest vertex probability requirement but pass all the remaining selection criteria. The muon charge misassignment is estimated to be less than 0.01% [27] and contributes a negligible uncertainty.

Final-state radiation is incorporated into the simulation using the PHOTOS algorithm. To estimate the systematic uncertainty associated with this procedure, the acceptance is calculated without FSR and 20% of the difference is taken as the uncertainty based on a study in Ref. [14] (0.8%).

The definition of acceptance used in this analysis requires that the muons from the Υ decay produce reconstructible tracks. The kinematic selection is applied to the reconstructed p_T and η values of these tracks. Uncertainties on the measurement of track parameters also affect the acceptance as a systematic uncertainty. The dominant uncertainty is associated with the measurement of the track transverse momentum. The acceptance is sensitive to biases in track momentum and to differences in resolution between the simulated and measured distributions. The magnitude of these effects is quantified by comparing measurements of resonance mass and width between simulation and data [19]. To determine the effect on the Υ acceptance, we introduce a track p_T bias of 0.2%, chosen to be 4 times the maximum momentum scale residual bias after calibration (0.3%). We also vary the transverse-momentum resolution by $\pm 10\%$, corresponding to the uncertainty in the resolution measurement using J/ψ, and recalculate the acceptance map (0.1%).

Imperfect knowledge of the production p_T spectrum of the Υ resonances at $\sqrt{s} = 7$ TeV contributes a systematic uncertainty. The Υ MC sample used for the acceptance calculation, Eq. (2), was generated flat in p_T, whereas the p_T spectrum in the data peaks at a few GeV/c, and behaves as a power law above 5 GeV/c. To study the effect of this difference, we have reweighted the sample in p_T to more closely describe the expected distribution in data based on a fit to the spectrum obtained from PYTHIA (1%).

The distribution of the z position of the pp interaction point influences the acceptance. We have produced MC samples of $\Upsilon(nS)$ at different positions along the beam line, between -10 and $+10$ cm with respect to the center of the nominal collision region (1%).

High-statistics MC simulations are performed to compare T&P single-muon and dimuon efficiencies to the actual MC values for both the Υ and J/ψ, see Figs. 3 and 4. The differences and their associated uncertainties are taken as a source of systematic uncertainty. The contributions are: possible bias in the T&P technique (0.1%), differences in the J/ψ and Υ kinematics (1%), and the possible misestimation of the double-muon Υ efficiency as the product of the single-muon efficiencies (1.6%).

Monte Carlo trials of the fitter demonstrate that it is consistent with providing an unbiased estimate of the yield

of each resonance, its mass, and the mass resolution (1%). A systematic variation may arise from differences between the dimuon invariant-mass distribution in the data and in the PDFs chosen for the signal and background components in the fit. We consider the following variations in the signal PDF. As the CB parameters which describe the radiative tail of each resonance are fixed from MC simulation in the nominal fit to the data, we vary the CB parameters by 3 times their uncertainties (3%). We also remove the resonance mass difference constraint in the p_{T} integrated fit (0.6%). We vary the background PDF by replacing the polynomial by a linear function, while restricting the fit to the mass range 8–12 GeV$/c^2$ (3% when fitting the full p_{T} and y ranges, varying with differential interval).

The determination of the integrated luminosity normalization is made with an uncertainty of 11% [9]. The relative systematic uncertainties from each source are summarized

TABLE VII. Relative values of the systematic uncertainties on the $\Upsilon(nS)$ production cross sections times the dimuon branching fraction, in p_{T} intervals for $|y| < 2$, assuming unpolarized production, in percent. The abbreviations used indicate the various systematic uncertainty sources: the statistical uncertainty in the estimation of the acceptance (A) and the trigger and muon identification efficiencies ($\varepsilon_{\mathrm{trig,id}}$); imperfect knowledge of the momentum scale (S_p), the production p_{T} spectrum ($A_{p_{\mathrm{T}}}$), the efficiency of the vertex-quality criterion (A_{vtx}), and the modeling of FSR (A_{FSR}); the use of the T&P method (T&P); the bias from using the J/ψ to determine single-muon efficiencies rather than the Υ ($\varepsilon_{J/\psi,\Upsilon}$); the background PDF (BG); the signal PDF, the fitter, the tracking efficiency, and effects arising from the efficiency binning (add). Values in parentheses denote the negative part of the asymmetric uncertainty. The luminosity uncertainty of 11% is not included in the table.

p_{T} (GeV$/c$)	A	$\varepsilon_{\mathrm{trig,id}}$	S_p	$A_{p_{\mathrm{T}}}$	A_{vtx}	A_{FSR}	T&P	$\varepsilon_{J/\psi,\Upsilon}$	BG	add.
	$\Upsilon(1S)$	$\lvert y\rvert < 2$				uncertainties are in percent				
0–30	0.5(0.5)	7.5(4.6)	0.3(0.3)	0.6	0.7	0.7	0.0	0.9	0.5	3.0
0–1	0.4(0.4)	8.3(5.4)	0.1(0.1)	0.2	1.1	0.8	0.5	0.8	3.4	3.1
1–2	0.4(0.4)	7.8(5.2)	0.2(0.2)	0.6	0.6	0.7	0.2	1.1	1.8	3.0
2–3	0.5(0.5)	7.3(4.7)	0.6(0.6)	0.3	0.3	0.8	0.1	1.1	1.5	3.0
3–4	0.6(0.6)	7.3(4.8)	0.6(0.6)	0.1	0.4	0.8	0.0	1.1	3.7	3.0
4–5	0.6(0.6)	7.4(4.5)	0.4(0.3)	0.3	0.7	0.7	0.0	0.9	2.3	3.0
5–6	0.6(0.6)	7.4(4.3)	0.2(0.3)	0.5	1.0	0.7	0.0	0.7	0.5	3.0
6–7	0.6(0.6)	7.4(4.1)	0.2(0.3)	0.7	1.1	0.6	0.1	0.7	0.4	3.0
7–8	0.6(0.6)	7.7(4.7)	0.1(0.1)	1.0	0.7	0.6	0.2	0.8	1.0	3.1
8–9	0.6(0.6)	7.4(4.2)	0.0(0.1)	1.2	0.7	0.5	0.0	0.7	1.0	3.0
9–10	0.5(0.5)	7.8(4.3)	0.1(0.0)	1.3	0.9	0.5	0.2	0.6	1.9	3.1
10–12	0.5(0.5)	7.4(3.7)	0.1(0.1)	1.4	0.8	0.5	0.2	0.6	0.2	3.0
12–14	0.5(0.4)	7.9(4.0)	0.2(0.1)	1.6	0.9	0.5	0.1	0.6	0.3	3.1
14–17	0.4(0.4)	8.5(4.2)	0.1(0.1)	1.6	0.9	0.5	0.3	0.6	2.2	3.1
17–20	0.4(0.4)	8.9(4.4)	0.1(0.1)	1.8	0.8	0.4	0.5	0.7	0.1	3.6
20–30	0.3(0.3)	8.9(4.3)	0.1(0.1)	1.6	0.7	0.5	0.3	0.6	0.1	3.5
	$\Upsilon(2S)$					$\lvert y\rvert < 2$				
0–30	0.6(0.6)	8.3(4.9)	0.3(0.3)	0.7	0.8	0.8	0.0	1.0	1.9	3.2
0–2	0.5(0.5)	8.3(5.2)	0.2(0.2)	0.5	0.6	0.8	0.4	0.6	6.8	3.3
2–4	0.7(0.7)	8.3(5.4)	0.7(0.8)	0.2	0.3	1.0	0.1	1.5	8.0	3.3
4–6	0.8(0.7)	7.9(4.7)	0.4(0.4)	0.4	1.1	0.8	0.0	0.9	5.2	3.3
6–9	0.7(0.7)	8.6(4.8)	0.1(0.1)	1.0	1.2	0.7	0.2	0.9	1.7	3.5
9–12	0.5(0.5)	8.4(4.2)	0.1(0.1)	1.5	1.0	0.5	0.2	0.8	0.9	3.6
12–16	0.4(0.5)	8.8(4.6)	0.1(0.1)	1.6	0.9	0.5	0.3	0.8	2.0	4.0
16–20	0.3(0.4)	8.3(4.1)	0.2(0.1)	1.7	1.0	0.5	0.4	0.5	0.0	6.5
20–30	0.3(0.3)	9.1(4.4)	0.1(0.1)	1.7	0.8	0.5	0.2	0.3	0.0	17.3
	$\Upsilon(3S)$					$\lvert y\rvert < 2$				
0–30	0.7(0.6)	8.6(4.7)	0.3(0.3)	0.8	0.8	0.8	0.1	1.0	3.4	5.4
0–3	0.5(0.5)	8.5(4.4)	0.4(0.5)	0.5	0.4	0.9	0.2	0.6	1.7	5.7
3–6	0.9(0.8)	9.1(5.4)	0.7(0.7)	0.3	0.9	1.0	0.0	1.7	14.1	7.3
6–9	0.7(0.7)	8.9(4.8)	0.2(0.2)	1.1	1.0	0.7	0.0	1.0	2.2	5.6
9–14	0.5(0.5)	7.5(4.1)	0.1(0.1)	1.5	0.8	0.5	0.3	0.7	0.4	6.1
14–20	0.4(0.4)	8.8(4.5)	0.2(0.1)	1.7	0.8	0.5	0.3	0.6	3.4	5.9
20–30	0.3(0.3)	8.8(4.1)	0.1(0.1)	1.6	0.8	0.5	0.5	0.5	0.3	8.3

TABLE VIII. Relative values of the systematic uncertainties on the $\Upsilon(nS)$ production cross sections times the dimuon branching fraction, in p_T intervals for $|y| < 1$ and $1 < |y| < 2$, assuming unpolarized production, in percent. The abbreviations used indicate the various systematic uncertainty sources: the statistical uncertainty in the estimation of the acceptance (A) and the trigger and muon identification efficiencies ($\varepsilon_{\text{trig,id}}$); imperfect knowledge of the momentum scale (S_p), the production p_T spectrum (A_{p_T}), the efficiency of the vertex-quality criterion (A_{vtx}), and the modeling of FSR (A_{FSR}); the use of the T&P method (T&P); the bias from using the J/ψ to determine single-muon efficiencies rather than the Υ ($\varepsilon_{J/\psi,\Upsilon}$); the background PDF (BG); the signal PDF, the fitter, the tracking efficiency, and effects arising from the efficiency binning (add). Values in parentheses denote the negative part of the asymmetric uncertainty. The luminosity uncertainty of 11% is not included in the table.

p_T (GeV/c)	A	$\varepsilon_{\text{trig,id}}$	S_p	A_{p_T}	A_{vtx}	A_{FSR}	T&P	$\varepsilon_{J/\psi,\Upsilon}$	BG	add.
	$\Upsilon(1S)$	$\|y\| < 1$				uncertainties are in percent				
0–30	0.5(0.5)	7.5(4.6)	0.3(0.3)	0.6	0.7	0.7	0.0	0.9	0.5	3.0
0–2	0.4(0.4)	7.7(5.6)	0.3(0.3)	0.6	0.5	0.7	0.7	1.3	1.6	3.0
2–5	0.6(0.6)	7.1(5.2)	0.7(0.7)	0.2	0.1	0.9	0.3	1.5	6.2	3.0
5–8	0.7(0.7)	6.5(4.4)	0.3(0.3)	0.8	0.8	0.7	0.4	1.0	0.3	3.0
8–11	0.5(0.5)	6.4(3.9)	0.0(0.0)	1.3	0.5	0.5	0.3	0.7	0.6	3.0
11–15	0.5(0.4)	6.6(3.8)	0.1(0.1)	1.5	0.7	0.5	0.3	0.6	0.4	3.0
15–30	0.3(0.4)	7.1(4.2)	0.1(0.2)	1.6	0.6	0.5	0.3	0.5	0.9	3.0
	$\Upsilon(2S)$					$\|y\| < 1$				
0–30	0.6(0.6)	8.3(4.9)	0.3(0.3)	0.7	0.8	0.8	0.0	1.0	1.9	3.2
0–3	0.6(0.5)	8.2(6.0)	0.6(0.6)	0.5	0.1	1.0	0.7	1.4	13.9	3.4
3–7	0.8(0.8)	7.7(5.2)	0.6(0.7)	0.4	0.6	1.0	0.4	1.5	13.1	3.4
7–11	0.6(0.6)	7.7(4.9)	0.1(0.0)	1.3	0.8	0.6	0.3	1.0	1.7	3.4
11–15	0.5(0.5)	7.3(4.4)	0.1(0.1)	1.6	0.8	0.5	0.3	0.7	1.6	3.6
15–30	0.3(0.4)	7.4(4.3)	0.1(0.2)	1.7	0.5	0.5	0.2	0.4	1.9	4.2
	$\Upsilon(3S)$					$\|y\| < 1$				
0–30	0.7(0.6)	8.6(4.7)	0.3(0.3)	0.8	0.8	0.8	0.1	1.0	3.4	5.4
0–7	0.8(0.8)	8.8(5.9)	0.6(0.7)	0.5	0.5	1.0	0.5	1.7	22.9	5.4
7–12	0.6(0.6)	7.6(5.0)	0.0(0.0)	1.4	0.6	0.6	0.1	0.9	2.2	5.7
12–30	0.4(0.4)	7.1(4.0)	0.2(0.1)	1.6	0.7	0.5	0.3	0.5	0.2	6.0
	$\Upsilon(1S)$					$1 < \|y\| < 2$				
0–30	0.5(0.5)	7.5(4.6)	0.3(0.3)	0.6	0.7	0.7	0.0	0.9	0.5	3.0
0–2	0.4(0.4)	8.2(4.6)	0.0(0.1)	0.3	1.1	0.6	0.2	0.6	7.3	3.0
2–5	0.5(0.5)	7.7(4.0)	0.3(0.3)	0.2	0.9	0.7	0.3	0.5	4.3	3.0
5–8	0.6(0.6)	8.4(4.2)	0.1(0.2)	0.7	1.2	0.6	0.5	0.6	0.4	3.0
8–11	0.6(0.5)	8.9(4.4)	0.0(0.1)	1.3	1.1	0.5	0.6	0.7	1.7	3.1
11–15	0.4(0.5)	9.1(4.2)	0.1(0.2)	1.6	0.9	0.5	0.8	0.6	0.1	3.0
15–30	0.4(0.5)	10.6(4.3)	0.2(0.3)	1.7	1.1	0.5	0.9	0.8	2.0	3.1
	$\Upsilon(2S)$					$1 < \|y\| < 2$				
0–30	0.6(0.6)	8.3(4.9)	0.3(0.3)	0.7	0.8	0.8	0.0	1.0	1.9	3.3
0–3	0.5(0.5)	7.8(3.8)	0.2(0.2)	0.3	1.2	0.7	0.2	0.5	21.9	3.8
3–7	0.7(0.7)	9.4(4.9)	0.3(0.3)	0.4	1.3	0.8	0.4	0.6	5.4	3.4
7–11	0.6(0.6)	9.6(4.8)	0.0(0.0)	1.2	1.1	0.6	0.7	0.8	4.4	3.5
11–15	0.5(0.5)	9.7(4.8)	0.1(0.2)	1.6	0.9	0.5	1.1	0.7	1.5	4.6
15–30	0.4(0.4)	9.5(3.8)	0.2(0.2)	1.7	1.3	0.4	1.0	0.7	3.4	7.2
	$\Upsilon(3S)$					$1 < \|y\| < 2$				
0–30	0.7(0.6)	8.6(4.7)	0.3(0.3)	0.8	0.8	0.8	0.1	1.0	3.4	5.5
0–7	0.7(0.6)	8.6(2.9)	0.4(0.4)	0.4	1.1	0.8	0.5	0.3	26.5	6.5
7–12	0.7(0.6)	9.3(4.1)	0.0(0.0)	1.3	1.0	0.6	1.1	0.6	6.2	6.7
12–30	0.4(0.4)	9.4(4.3)	0.1(0.2)	1.7	1.1	0.5	0.9	0.5	1.5	5.9

in Table VII for the full rapidity range, for two rapidity ranges in Table VIII, and for five rapidity ranges in Table IX. The largest sources of systematic uncertainty arise from the statistical precision of the efficiency measurements from data and from the luminosity normalization, with the latter dominating.

VIII. RESULTS AND DISCUSSION

The analysis of the collision data acquired by the CMS experiment at $\sqrt{s} = 7$ TeV, corresponding to an integrated luminosity of 3.1 ± 0.3 pb^{-1}, yields a measurement of the $\Upsilon(nS)$ integrated production cross sections for the range $|y| < 2$:

TABLE IX. Relative values of the systematic uncertainties on the $\Upsilon(1S)$ production cross section times the dimuon branching fraction, in rapidity intervals for $p_T < 30$ GeV$/c$, assuming unpolarized production, in percent. The abbreviations used indicate the various systematic uncertainty sources: the statistical uncertainty in the estimation of the acceptance (A) and the trigger and muon identification efficiencies ($\varepsilon_{\text{trig,id}}$); imperfect knowledge of the momentum scale (S_p), the production p_T spectrum (A_{p_T}), the efficiency of the vertex-quality criterion (A_{vtx}), and the modeling of FSR (A_{FSR}); the use of the T&P method (T&P); the bias from using the J/ψ to determine single-muon efficiencies rather than the Υ ($\varepsilon_{J/\psi,\Upsilon}$); the background PDF (BG); the signal PDF, the fitter, the tracking efficiency, and effects arising from the efficiency binning (add). Values in parentheses denote the negative part of the asymmetric uncertainty. The luminosity uncertainty of 11% is not included in the table.

$\lvert y\rvert$	A $\Upsilon(1S)$	$\varepsilon_{\text{trig,id}}$ $p_T < 30$ GeV$/c$	S_p	A_{p_T}	A_{vtx}	A_{FSR}	T&P	$\varepsilon_{J/\psi,\Upsilon}$	BG	add.
					uncertainties are in percent					
0.0–2.0	0.5	7.5(4.6)	0.3(0.3)	0.6	0.7	0.7	0.0	0.9	0.5	3.0
0.0–0.4	0.6	6.8(4.9)	0.4(0.4)	0.7	0.3	0.7	0.6	1.5	0.1	3.0
0.4–0.8	0.6	6.8(4.7)	0.4(0.4)	0.6	0.3	0.7	0.3	1.1	5.4	3.0
0.8–1.2	0.5	7.5(4.9)	0.3(0.3)	0.6	1.0	0.7	0.1	0.7	2.9	3.0
1.2–1.6	0.5	7.7(4.0)	0.2(0.2)	0.6	1.2	0.6	0.2	0.5	4.0	3.0
1.6–2.0	0.6	9.3(4.0)	0.0(0.1)	0.6	0.9	0.6	0.9	0.6	5.0	3.0

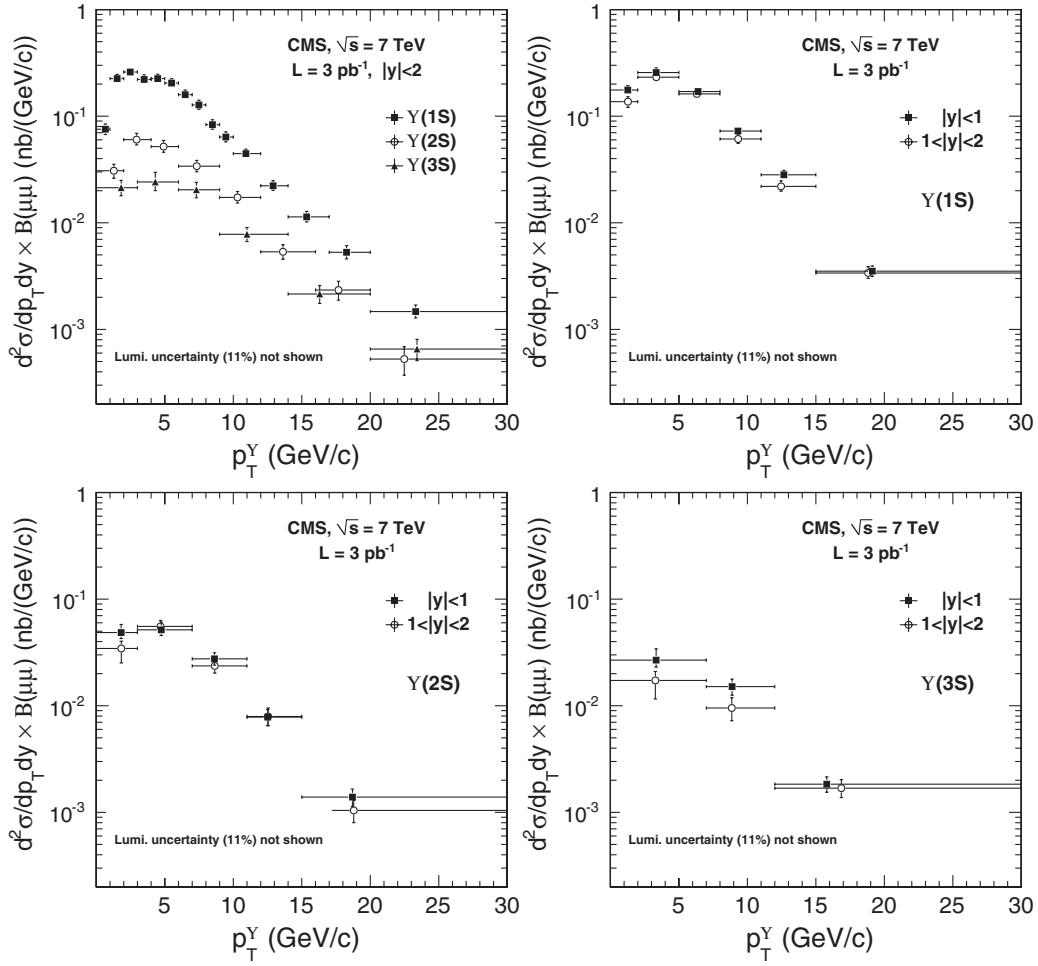


FIG. 7. $\Upsilon(nS)$ differential cross sections in the rapidity interval $|y| < 2$ (top left), and in the rapidity intervals $|y| < 1$ and $1 < |y| < 2$ for the $\Upsilon(1S)$ (top right), $\Upsilon(2S)$ (bottom left) and $\Upsilon(3S)$ (bottom right). The uncertainties on the points represent the sum of the statistical and systematic uncertainties added in quadrature, excluding the uncertainty on the integrated luminosity (11%).

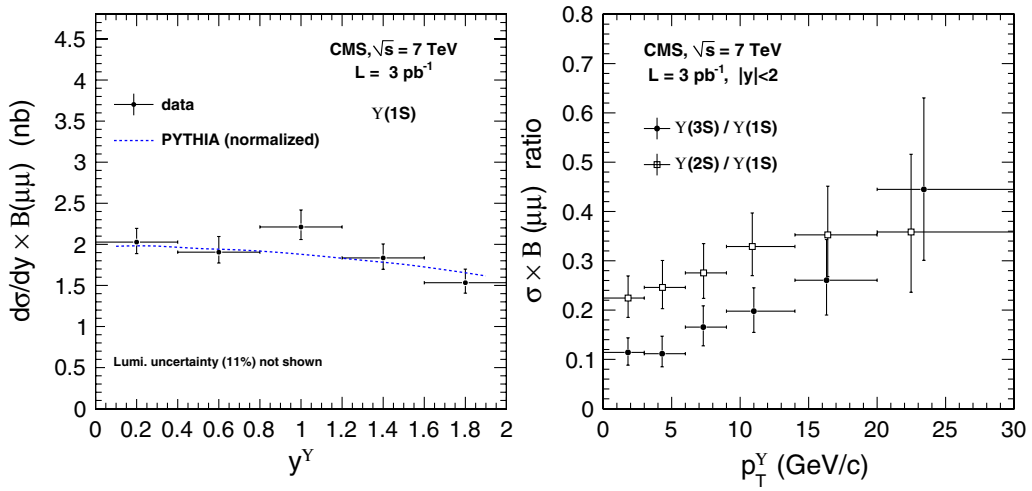


FIG. 8 (color online). (Left) Differential $\Upsilon(1S)$ cross section as a function of rapidity in the transverse-momentum range $p_T < 30$ GeV$/c$ (data points) and normalized PYTHIA prediction (line). The uncertainties on the points represent the sum of the statistical and systematic uncertainties added in quadrature, excluding the uncertainty on the integrated luminosity (11%). (Right) Cross section ratios for $\Upsilon(nS)$ states as a function of p_T in the rapidity range $|y| < 2$.

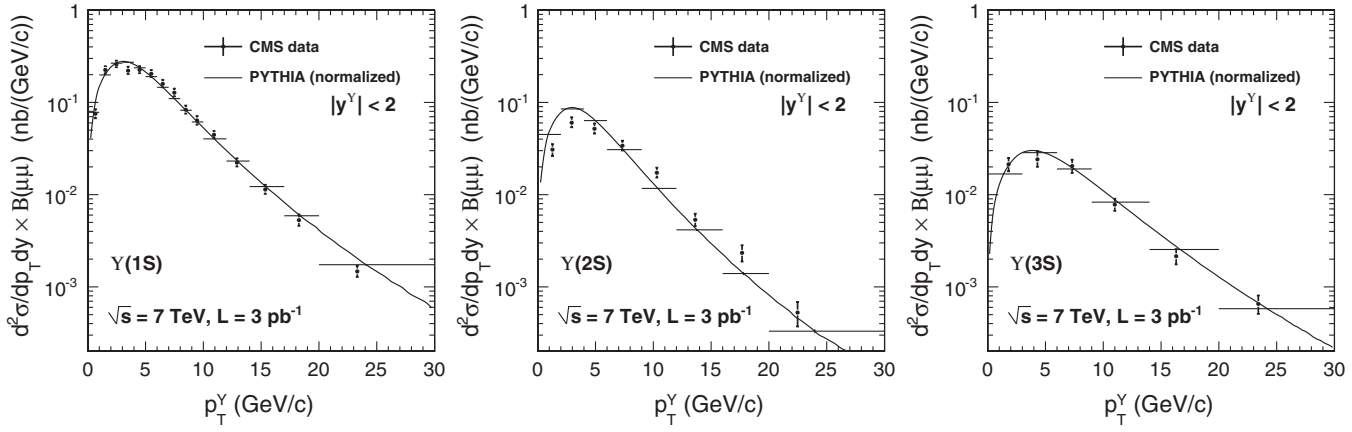


FIG. 9. Differential cross sections of the $\Upsilon(nS)$ as a function of p_T in the rapidity range $|y| < 2$, and comparison to the PYTHIA predictions normalized to the measured p_T-integrated cross sections; $\Upsilon(1S)$ (left), $\Upsilon(2S)$ (middle), and $\Upsilon(3S)$ (right). The theory prediction is shown in the form of a continuous spectrum (curve) and integrated in the same p_T bins as employed in the measurement (horizontal lines). The PYTHIA curve is used to calculate the abscissa of the data points [28]. The uncertainties on the points represent the sum of the statistical and systematic uncertainties added in quadrature, excluding the uncertainty on the integrated luminosity (11%).

TABLE X. The ratios of $\Upsilon(nS)$ cross sections for different Υ p_T ranges in the unpolarized scenario. The first uncertainty is statistical and the second is systematic. The ratios are independent of the luminosity normalization and its uncertainty.

p_T (GeV$/c$)	$\Upsilon(3S)/\Upsilon(1S)$	$\Upsilon(2S)/\Upsilon(1S)$
0–30	$0.14 \pm 0.01 \pm 0.02$	$0.26 \pm 0.02 \pm 0.04$
0–3	$0.11 \pm 0.02 \pm 0.02$	$0.22 \pm 0.03 \pm 0.04$
3–6	$0.11 \pm 0.02 \pm 0.03$	$0.25 \pm 0.03 \pm 0.05$
6–9	$0.17 \pm 0.03 \pm 0.03$	$0.28 \pm 0.04 \pm 0.04$
9–14	$0.20 \pm 0.03 \pm 0.03$	$0.33 \pm 0.04 \pm 0.05$
14–20	$0.26 \pm 0.07 \pm 0.04$	$0.35 \pm 0.08 \pm 0.05$
20–30	$0.44 \pm 0.16 \pm 0.08$	$0.36 \pm 0.14 \pm 0.06$

$$\sigma(pp \to \Upsilon(1S)X) \cdot \mathcal{B}(\Upsilon(1S) \to \mu^+\mu^-) = 7.37 \pm 0.13(\text{stat.})(\text{syst.}) \pm 0.81(\text{lumi.})\ \text{nb},$$

$$\sigma(pp \to \Upsilon(2S)X) \cdot \mathcal{B}(\Upsilon(2S) \to \mu^+\mu^-) = 1.90 \pm 0.08(\text{stat.})(\text{syst.}) \pm 0.21(\text{lumi.})\ \text{nb},$$

$$\sigma(pp \to \Upsilon(3S)X) \cdot \mathcal{B}(\Upsilon(3S) \to \mu^+\mu^-) = 1.02 \pm 0.07(\text{stat.})(\text{syst.}) \pm 0.11(\text{lumi.})\ \text{nb}.$$

$$- 0.08 + 0.11 - 0.12 + 0.18 - 0.42 + 0.61$$

The $\Upsilon(1S)$ and $\Upsilon(2S)$ measurements include feed-down from higher-mass states, such as the χ_b family and the $\Upsilon(3S)$. These measurements assume unpolarized $\Upsilon(nS)$

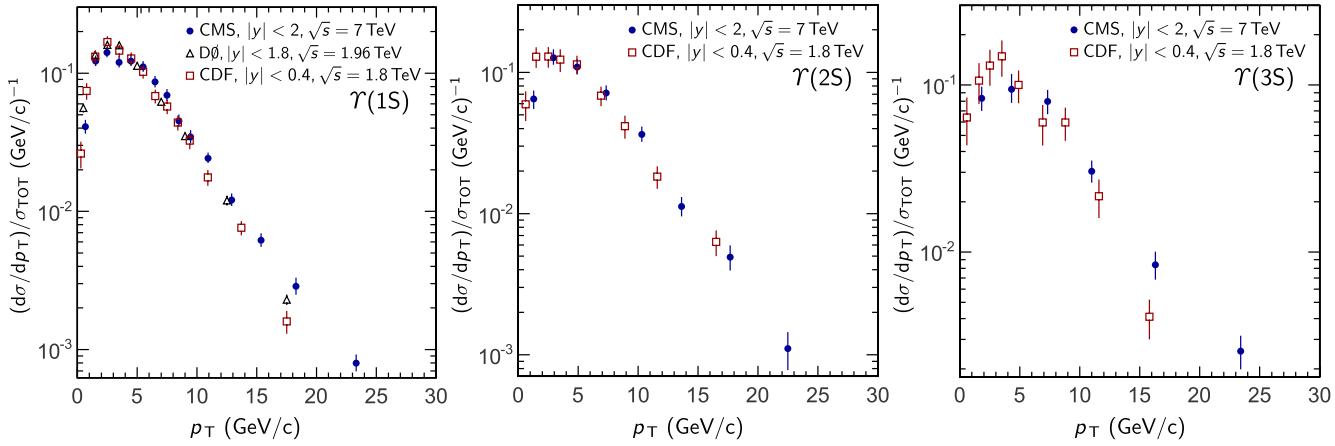


FIG. 10 (color online). Comparison of the CMS differential $\Upsilon(nS)$ cross sections as a function of p_T, normalized by $\sigma_{TOT} = \sum(d\sigma/dp_T)\Delta p_T$, to previous measurements; $\Upsilon(1S)$ (left), $\Upsilon(2S)$ (middle), and $\Upsilon(3S)$ (right).

production. Assumptions of fully-transverse or fully-longitudinal polarizations change the measured cross section values by about 20%. The differential $\Upsilon(nS)$ cross sections as a function of p_T for the rapidity intervals $|y| < 1$, $1 < |y| < 2$, and $|y| < 2$ are shown in Fig. 7. The p_T dependence of the cross section in the two exclusive rapidity intervals is the same within the uncertainties. The $\Upsilon(1S)$ differential cross sections as a function of rapidity and integrated in p_T are shown in the left plot of Fig. 8. The cross section shows a slight decline towards $|y| = 2$, consistent with the expectation from PYTHIA. The ratios of $\Upsilon(nS)$ differential cross sections as a function of p_T are reported in Table X and shown in the right plot of Fig. 8. The uncertainty associated with the luminosity determination cancels in the computation of the ratios. Both ratios increase with p_T. In Fig. 9 the differential cross sections for the $\Upsilon(1S)$, $\Upsilon(2S)$, and $\Upsilon(3S)$ are compared to PYTHIA. The normalized p_T-spectrum prediction from PYTHIA is consistent with the measurements, while the integrated cross section is overestimated by about a factor of 2. We have not included parameter uncertainties in the PYTHIA calculation. We do not compare our measurements to other models as no published predictions exist at $\sqrt{s} = 7$ TeV for Υ production.

The $\Upsilon(nS)$ integrated cross sections are expected to increase with $\sqrt{s}$. As the gluon-gluon amplitude is expected to dominate production of Υ resonances at both the LHC and the Tevatron, we compare, in Table XI, our measurement of the $\Upsilon(1S)$ integrated cross section in the central rapidity region $|y| < 1$ to previous measurements [4,5] performed in $p\bar{p}$ collisions. Previous measurements were performed in the range $p_T < 20$ GeV/c, and $|y| < 0.4$ for CDF and $|y| < 1.8$ for DØ. Under the assumption that the cross section is uniform in rapidity for the measurement range of each experiment, the cross section we measure at $\sqrt{s} = 7$ TeV is about 3 times larger than the cross section measured at the Tevatron. Although our measurement extends to higher p_T than the Tevatron measurements, the fraction of the cross section satisfying $p_T > 20$ GeV/c is less than 1% and so can be neglected for this comparison. We compare the normalized differential cross sections in p_T at the Tevatron to our measurements in Fig. 10.

TABLE XI. $\Upsilon(1S)$ cross section measurements at several center-of-mass collision energies from the Tevatron ($p\bar{p}$) experiments CDF and D0 and from CMS (pp). The first uncertainty is statistical, the second is systematic, and the third is associated with the luminosity determination.

Exp.	$\sqrt{s}$ (TeV)	$\sigma(p^{(-)}\bar{p} \to \Upsilon(1S)X) \times \frac{1}{\Delta y} \times B(\Upsilon \to \mu\mu)$	rapidity range
CDF	1.8	$0.680 \pm 0.015 \pm 0.018 \pm 0.026$ nb [4]	$\|y\| < 0.4$
D0	1.96	$0.628 \pm 0.016 \pm 0.065 \pm 0.038$ nb [5]	$\|y\| < 0.6$
CMS	7.0	$2.02 \pm 0.03^{+0.16}_{-0.12} \pm 0.22$ nb (this work)	$\|y\| < 1.0$

IX. SUMMARY

The study of the $\Upsilon(nS)$ resonances provides important information on the process of hadroproduction of heavy quarks. In this paper we have presented the first measurement of the $\Upsilon(nS)$ differential production cross section for proton-proton collisions at $\sqrt{s} = 7$ TeV. Integrated over the range $p_T < 30$ GeV/c and $|y| < 2$, we find the product of the $\Upsilon(1S)$ production cross section and dimuon branching fraction to be $\sigma(pp \to \Upsilon(1S)X) \cdot \mathcal{B}(\Upsilon(1S) \to \mu^+\mu^-) = 7.37 \pm 0.13^{+0.61}_{-0.42} \pm 0.81$ nb, where the first uncertainty is statistical, the second is systematic, and the third is associated with the estimation of the integrated luminosity of the data sample. Under the assumption that the cross section is uniform in rapidity for the measurement range of each experiment, the cross section we measure at $\sqrt{s} = 7$ TeV is about 3 times larger than the cross section measured at the Tevatron. The $\Upsilon(2S)$ and $\Upsilon(3S)$ integrated cross sections and the $\Upsilon(1S)$, $\Upsilon(2S)$, and $\Upsilon(3S)$ differential cross sections in transverse-momentum in two regions of rapidity have also been determined. The differential cross

section measurements have been compared to previous measurements and PYTHIA. Finally, the cross section ratios of the three $\Upsilon(nS)$ have been measured.

The dominant sources of systematic uncertainty on the cross-section measurement arise from the tag-and-probe determination of the efficiencies and from the integrated luminosity normalization. Both will be reduced with additional data. Assuming fully-transverse or fully-longitudinal production polarization instead of unpolarized $\Upsilon(nS)$ production changes the cross-section measurements by about 20%. With a larger accumulated data sample, it will become possible to perform a simultaneous measurement of the polarization and the cross section. This work provides new experimental results which will serve as input to ongoing theoretical investigations of the correct description of bottomonium production.

ACKNOWLEDGMENTS

We wish to congratulate our colleagues in the CERN accelerator departments for the excellent performance of the LHC machine. We thank the technical and administrative staff at CERN and other CMS institutes. This work was supported by the Austrian Federal Ministry of Science and Research; the Belgium Fonds de la Recherche Scientifique, and Fonds voor Wetenschappelijk Onderzoek; the Brazilian Funding Agencies (CNPq, CAPES, FAPERJ, and FAPESP); the Bulgarian Ministry of Education and Science; CERN; the Chinese Academy of Sciences, Ministry of Science and Technology, and National Natural Science Foundation of China; the Colombian Funding Agency (COLCIENCIAS); the Croatian Ministry of Science, Education and Sport; the Research Promotion Foundation, Cyprus; the Estonian Academy of Sciences and NICPB; the Academy of Finland, Finnish Ministry of Education, and Helsinki Institute of Physics; the Institut National de Physique Nucléaire et de Physique des Particules/CNRS, and Commissariat à l'Énergie Atomique et aux Énergies Alternatives/CEA, France; the Bundesministerium für Bildung und Forschung, Deutsche Forschungsgemeinschaft, and Helmholtz-Gemeinschaft Deutscher Forschungszentren, Germany; the General Secretariat for Research and Technology, Greece; the National Scientific Research Foundation, and National Office for Research and Technology, Hungary; the Department of Atomic Energy, and Department of Science and Technology, India; the Institute for Studies in Theoretical Physics and Mathematics, Iran; the Science Foundation, Ireland; the Istituto Nazionale di Fisica Nucleare, Italy; the Korean Ministry of Education, Science and Technology and the World Class University program of NRF, Korea; the Lithuanian Academy of Sciences; the Mexican Funding Agencies (CINVESTAV, CONACYT, SEP, and UASLP-FAI); the Pakistan Atomic Energy Commission; the State Commission for Scientific Research, Poland; the Fundação para a Ciência e a Tecnologia, Portugal; JINR (Armenia, Belarus, Georgia, Ukraine, Uzbekistan); the Ministry of Science and Technologies of the Russian Federation, and Russian Ministry of Atomic Energy; the Ministry of Science and Technological Development of Serbia; the Ministerio de Ciencia e Innovación, and Programa Consolider-Ingenio 2010, Spain; the Swiss Funding Agencies (ETH Board, ETH Zurich, PSI, SNF, UniZH, Canton Zurich, and SER); the National Science Council, Taipei; the Scientific and Technical Research Council of Turkey, and Turkish Atomic Energy Authority; the Science and Technology Facilities Council, UK; the US Department of Energy, and the US National Science Foundation. Individuals have received support from the Marie-Curie programme and the European Research Council (European Union); the Leventis Foundation; the A. P. Sloan Foundation; the Alexander von Humboldt Foundation; the Associazione per lo Sviluppo Scientifico e Tecnologico del Piemonte (Italy); the Belgian Federal Science Policy Office; the Fonds pour la Formation à la Recherche dans l'Industrie et dans l'Agriculture (FRIA-Belgium); and the Agentschap voor Innovatie door Wetenschap en Technologie (IWT-Belgium).

[1] N. Brambilla *et al.*, Report No. CERN-2005-005, 2004, http://cdsweb.cern.ch/record/872545.
[2] G. T. Bodwin, E. Braaten, and G. P. Lepage, Phys. Rev. D **51**, 1125 (1995).
[3] P. Artoisenet *et al.*, Phys. Rev. Lett. **101**, 152001 (2008).
[4] D. E. Acosta *et al.* (CDF), Phys. Rev. Lett. **88**, 161802 (2002).
[5] V. M. Abazov *et al.* (D0), Phys. Rev. Lett. **94**, 232001 (2005); **100**, 049902(E) (2008).
[6] T. Sjöstrand, S. Mrenna, and P. Z. Skands, J. High Energy Phys. 05 (2006) 026.
[7] CMS Collaboration, JINST **5**, T03009 (2010).
[8] CMS Collaboration, JINST **3**, S08004 (2008).
[9] CMS Collaboration, CMS-PAS-EWK-10-004, 2010, http://cdsweb.cern.ch/record/1279145.
[10] CMS Collaboration, Eur. Phys. J. C **70**, 1165 (2010).
[11] M. Krämer, Prog. Part. Nucl. Phys. **47**, 141 (2001).
[12] M. Bargiotti and V. Vagnoni, Report No. LHCb-2007-042, 2007, http://cdsweb.cern.ch/record/1042611.
[13] E. Barberio, B. van Eijk, and Z. Wąs, Comput. Phys. Commun. **66**, 115 (1991).
[14] E. Barberio and Z. Was, Comput. Phys. Commun. **79**, 291 (1994).

[15] S. Agostinelli *et al.*, Nucl. Instrum. Methods Phys. Res., Sect. A **506**, 250 (2003).
[16] CMS Collaboration, Report No. CMS-PAS-MUO-10-002, 2010, http://cdsweb.cern.ch/record/1279140.
[17] CMS Collaboration, JINST **5**, T03021 (2010).
[18] CMS Collaboration, Report No. CMS-PAS-TRK-10-003, 2010, http://cdsweb.cern.ch/record/1279138.
[19] CMS Collaboration, Report No. CMS-PAS-TRK-10-004, 2010, http://cdsweb.cern.ch/record/1279137.
[20] D. J. Lange, Nucl. Instrum. Methods Phys. Res., Sect. A **462**, 152 (2001).
[21] P. Faccioli *et al.*, Eur. Phys. J. C **69**, 657 (2010).
[22] J. C. Collins and D. E. Soper, Phys. Rev. D **16**, 2219 (1977).
[23] CMS Collaboration, Report No. CMS-PAS-TRK-10-002, 2010, http://cdsweb.cern.ch/record/1279139 .
[24] CMS Collaboration, Eur. Phys. J. C **71**, 1575 (2011).
[25] M. J. Oreglia, Ph.D. thesis, Stanford University 1980] http://www.slac.stanford.edu/pubs/slacreports/slac-r-236.html.
[26] K. Nakamura *et al.* (Particle Data Group), J. Phys. G **37**, 075021 (2010).
[27] CMS Collaboration, JINST **5**, T03022 (2010).
[28] G. D. Lafferty and T. R. Wyatt, Nucl. Instrum. Methods Phys. Res., Sect. A **355**, 541 (1995).

V. Khachatryan,[1] A. M. Sirunyan,[1] A. Tumasyan,[1] W. Adam,[2] T. Bergauer,[2] M. Dragicevic,[2] J. Erö,[2] C. Fabjan,[2] M. Friedl,[2] R. Frühwirth,[2] V. M. Ghete,[2] J. Hammer,[2,b] S. Hänsel,[2] C. Hartl,[2] M. Hoch,[2] N. Hörmann,[2] J. Hrubec,[2] M. Jeitler,[2] G. Kasieczka,[2] W. Kiesenhofer,[2] M. Krammer,[2] D. Liko,[2] I. Mikulec,[2] M. Pernicka,[2] H. Rohringer,[2] R. Schöfbeck,[2] J. Strauss,[2] A. Taurok,[2] F. Teischinger,[2] W. Waltenberger,[2] G. Walzel,[2] E. Widl,[2] C.-E. Wulz,[2] V. Mossolov,[3] N. Shumeiko,[3] J. Suarez Gonzalez,[3] L. Benucci,[4] L. Ceard,[4] K. Cerny,[4] E. A. De Wolf,[4] X. Janssen,[4] T. Maes,[4] L. Mucibello,[4] S. Ochesanu,[4] B. Roland,[4] R. Rougny,[4] M. Selvaggi,[4] H. Van Haevermaet,[4] P. Van Mechelen,[4] N. Van Remortel,[4] V. Adler,[5] S. Beauceron,[5] F. Blekman,[5] S. Blyweert,[5] J. D'Hondt,[5] O. Devroede,[5] R. Gonzalez Suarez,[5] A. Kalogeropoulos,[5] J. Maes,[5] M. Maes,[5] S. Tavernier,[5] W. Van Doninck,[5] P. Van Mulders,[5] G. P. Van Onsem,[5] I. Villella,[5] O. Charaf,[6] B. Clerbaux,[6] G. De Lentdecker,[6] V. Dero,[6] A. P. R. Gay,[6] G. H. Hammad,[6] T. Hreus,[6] P. E. Marage,[6] L. Thomas,[6] C. Vander Velde,[6] P. Vanlaer,[6] J. Wickens,[6] S. Costantini,[7] M. Grunewald,[7] B. Klein,[7] A. Marinov,[7] J. Mccartin,[7] D. Ryckbosch,[7] F. Thyssen,[7] M. Tytgat,[7] L. Vanelderen,[7] P. Verwilligen,[7] S. Walsh,[7] N. Zaganidis,[7] S. Basegmez,[8] G. Bruno,[8] J. Caudron,[8] J. De Favereau De Jeneret,[8] C. Delaere,[8] P. Demin,[8] D. Favart,[8] A. Giammanco,[8] G. Grégoire,[8] J. Hollar,[8] V. Lemaitre,[8] J. Liao,[8] O. Militaru,[8] S. Ovyn,[8] D. Pagano,[8] A. Pin,[8] K. Piotrzkowski,[8] L. Quertenmont,[8] N. Schul,[8] N. Beliy,[9] T. Caebergs,[9] E. Daubie,[9] G. A. Alves,[10] D. De Jesus Damiao,[10] M. E. Pol,[10] M. H. G. Souza,[10] W. Carvalho,[11] E. M. Da Costa,[11] C. De Oliveira Martins,[11] S. Fonseca De Souza,[11] L. Mundim,[11] H. Nogima,[11] V. Oguri,[11] W. L. Prado Da Silva,[11] A. Santoro,[11] S. M. Silva Do Amaral,[11] A. Sznajder,[11] F. A. Dias,[12] M. A. F. Dias,[12] T. R. Fernandez Perez Tomei,[12] E. M. Gregores,[12,c] F. Marinho,[12] S. F. Novaes,[12] Sandra S. Padula,[12] N. Darmenov,[13,b] L. Dimitrov,[13] V. Genchev,[13,b] P. Iaydjiev,[13,b] S. Piperov,[13] M. Rodozov,[13] S. Stoykova,[13] G. Sultanov,[13] V. Tcholakov,[13] R. Trayanov,[13] I. Vankov,[13] M. Dyulendarova,[14] R. Hadjiiska,[14] V. Kozhuharov,[14] L. Litov,[14] E. Marinova,[14] M. Mateev,[14] B. Pavlov,[14] P. Petkov,[14] J. G. Bian,[15] G. M. Chen,[15] H. S. Chen,[15] C. H. Jiang,[15] D. Liang,[15] S. Liang,[15] J. Wang,[15] J. Wang,[15] X. Wang,[15] Z. Wang,[15] M. Xu,[15] M. Yang,[15] J. Zang,[15] Z. Zhang,[15] Y. Ban,[16] S. Guo,[16] W. Li,[16] Y. Mao,[16] S. J. Qian,[16] H. Teng,[16] L. Zhang,[16] B. Zhu,[16] A. Cabrera,[17] B. Gomez Moreno,[17] A. A. Ocampo Rios,[17] A. F. Osorio Oliveros,[17] J. C. Sanabria,[17] N. Godinovic,[18] D. Lelas,[18] K. Lelas,[18] R. Plestina,[18,d] D. Polic,[18] I. Puljak,[18] Z. Antunovic,[19] M. Dzelalija,[19] V. Brigljevic,[20] S. Duric,[20] K. Kadija,[20] S. Morovic,[20] A. Attikis,[21] M. Galanti,[21] J. Mousa,[21] C. Nicolaou,[21] F. Ptochos,[21] P. A. Razis,[21] H. Rykaczewski,[21] Y. Assran,[22,e] M. A. Mahmoud,[22,f] A. Hektor,[23] M. Kadastik,[23] K. Kannike,[23] M. Müntel,[23] M. Raidal,[23] L. Rebane,[23] V. Azzolini,[24] P. Eerola,[24] S. Czellar,[25] J. Härkönen,[25] A. Heikkinen,[25] V. Karimäki,[25] R. Kinnunen,[25] J. Klem,[25] M. J. Kortelainen,[25] T. Lampén,[25] K. Lassila-Perini,[25] S. Lehti,[25] T. Lindén,[25] P. Luukka,[25] T. Mäenpää,[25] E. Tuominen,[25] J. Tuominiemi,[25] E. Tuovinen,[25] D. Ungaro,[25] L. Wendland,[25] K. Banzuzi,[26] A. Korpela,[26] T. Tuuva,[26] D. Sillou,[27] M. Besancon,[28] S. Choudhury,[28] M. Dejardin,[28] D. Denegri,[28] B. Fabbro,[28] J. L. Faure,[28] F. Ferri,[28] S. Ganjour,[28] F. X. Gentit,[28] A. Givernaud,[28] P. Gras,[28] G. Hamel de Monchenault,[28] P. Jarry,[28] E. Locci,[28] J. Malcles,[28] M. Marionneau,[28] L. Millischer,[28] J. Rander,[28] A. Rosowsky,[28] I. Shreyber,[28] M. Titov,[28] P. Verrecchia,[28] S. Baffioni,[29] F. Beaudette,[29] L. Bianchini,[29] M. Bluj,[29,g] C. Broutin,[29] P. Busson,[29] C. Charlot,[29] T. Dahms,[29] L. Dobrzynski,[29] R. Granier de Cassagnac,[29] M. Haguenauer,[29] P. Miné,[29] C. Mironov,[29] C. Ochando,[29] P. Paganini,[29] D. Sabes,[29] R. Salerno,[29] Y. Sirois,[29] C. Thiebaux,[29] B. Wyslouch,[29,h] A. Zabi,[29] J.-L. Agram,[30,i] J. Andrea,[30] A. Besson,[30] D. Bloch,[30] D. Bodin,[30] J.-M. Brom,[30] M. Cardaci,[30] E. C. Chabert,[30] C. Collard,[30] E. Conte,[30,i] F. Drouhin,[30,i] C. Ferro,[30] J.-C. Fontaine,[30,i] D. Gelé,[30] U. Goerlach,[30] S. Greder,[30] P. Juillot,[30] M. Karim,[30,i] A.-C. Le Bihan,[30] Y. Mikami,[30] P. Van Hove,[30] F. Fassi,[31] D. Mercier,[31] C. Baty,[32] N. Beaupere,[32]

M. Bedjidian,[32] O. Bondu,[32] G. Boudoul,[32] D. Boumediene,[32] H. Brun,[32] N. Chanon,[32] R. Chierici,[32] D. Contardo,[32] P. Depasse,[32] H. El Mamouni,[32] A. Falkiewicz,[32] J. Fay,[32] S. Gascon,[32] B. Ille,[32] T. Kurca,[32] T. Le Grand,[32] M. Lethuillier,[32] L. Mirabito,[32] S. Perries,[32] V. Sordini,[32] S. Tosi,[32] Y. Tschudi,[32] P. Verdier,[32] H. Xiao,[32] V. Roinishvili,[33] G. Anagnostou,[34] M. Edelhoff,[34] L. Feld,[34] N. Heracleous,[34] O. Hindrichs,[34] R. Jussen,[34] K. Klein,[34] J. Merz,[34] N. Mohr,[34] A. Ostapchuk,[34] A. Perieanu,[34] F. Raupach,[34] J. Sammet,[34] S. Schael,[34] D. Sprenger,[34] H. Weber,[34] M. Weber,[34] B. Wittmer,[34] M. Ata,[35] W. Bender,[35] M. Erdmann,[35] J. Frangenheim,[35] T. Hebbeker,[35] A. Hinzmann,[35] K. Hoepfner,[35] C. Hof,[35] T. Klimkovich,[35] D. Klingebiel,[35] P. Kreuzer,[35] D. Lanske,[35,a] C. Magass,[35] G. Masetti,[35] M. Merschmeyer,[35] A. Meyer,[35] P. Papacz,[35] H. Pieta,[35] H. Reithler,[35] S. A. Schmitz,[35] L. Sonnenschein,[35] J. Steggemann,[35] D. Teyssier,[35] M. Bontenackels,[36] M. Davids,[36] M. Duda,[36] G. Flügge,[36] H. Geenen,[36] M. Giffels,[36] W. Haj Ahmad,[36] D. Heydhausen,[36] T. Kress,[36] Y. Kuessel,[36] A. Linn,[36] A. Nowack,[36] L. Perchalla,[36] O. Pooth,[36] J. Rennefeld,[36] P. Sauerland,[36] A. Stahl,[36] M. Thomas,[36] D. Tornier,[36] M. H. Zoeller,[36] M. Aldaya Martin,[37] W. Behrenhoff,[37] U. Behrens,[37] M. Bergholz,[37,j] K. Borras,[37] A. Cakir,[37] A. Campbell,[37] E. Castro,[37] D. Dammann,[37] G. Eckerlin,[37] D. Eckstein,[37] A. Flossdorf,[37] G. Flucke,[37] A. Geiser,[37] I. Glushkov,[37] J. Hauk,[37] H. Jung,[37] M. Kasemann,[37] I. Katkov,[37] P. Katsas,[37] C. Kleinwort,[37] H. Kluge,[37] A. Knutsson,[37] D. Krücker,[37] E. Kuznetsova,[37] W. Lange,[37] W. Lohmann,[37,j] R. Mankel,[37] M. Marienfeld,[37] I.-A. Melzer-Pellmann,[37] A. B. Meyer,[37] J. Mnich,[37] A. Mussgiller,[37] J. Olzem,[37] A. Parenti,[37] A. Raspereza,[37] A. Raval,[37] R. Schmidt,[37,j] T. Schoerner-Sadenius,[37] N. Sen,[37] M. Stein,[37] J. Tomaszewska,[37] D. Volyanskyy,[37] R. Walsh,[37] C. Wissing,[37] C. Autermann,[38] S. Bobrovskyi,[38] J. Draeger,[38] H. Enderle,[38] U. Gebbert,[38] K. Kaschube,[38] G. Kaussen,[38] R. Klanner,[38] J. Lange,[38] B. Mura,[38] S. Naumann-Emme,[38] F. Nowak,[38] N. Pietsch,[38] C. Sander,[38] H. Schettler,[38] P. Schleper,[38] M. Schröder,[38] T. Schum,[38] J. Schwandt,[38] A. K. Srivastava,[38] H. Stadie,[38] G. Steinbrück,[38] J. Thomsen,[38] R. Wolf,[38] C. Barth,[39] J. Bauer,[39] V. Buege,[39] T. Chwalek,[39] W. De Boer,[39] A. Dierlamm,[39] G. Dirkes,[39] M. Feindt,[39] J. Gruschke,[39] C. Hackstein,[39] F. Hartmann,[39] S. M. Heindl,[39] M. Heinrich,[39] H. Held,[39] K. H. Hoffmann,[39] S. Honc,[39] T. Kuhr,[39] D. Martschei,[39] S. Mueller,[39] Th. Müller,[39] M. Niegel,[39] O. Oberst,[39] A. Oehler,[39] J. Ott,[39] T. Peiffer,[39] D. Piparo,[39] G. Quast,[39] K. Rabbertz,[39] F. Ratnikov,[39] M. Renz,[39] C. Saout,[39] A. Scheurer,[39] P. Schieferdecker,[39] F.-P. Schilling,[39] G. Schott,[39] H. J. Simonis,[39] F. M. Stober,[39] D. Troendle,[39] J. Wagner-Kuhr,[39] M. Zeise,[39] V. Zhukov,[39,k] E. B. Ziebarth,[39] G. Daskalakis,[40] T. Geralis,[40] S. Kesisoglou,[40] A. Kyriakis,[40] D. Loukas,[40] I. Manolakos,[40] A. Markou,[40] C. Markou,[40] C. Mavrommatis,[40] E. Petrakou,[40] L. Gouskos,[41] T. J. Mertzimekis,[41] A. Panagiotou,[41,b] I. Evangelou,[42] C. Foudas,[42] P. Kokkas,[42] N. Manthos,[42] I. Papadopoulos,[42] V. Patras,[42] F. A. Triantis,[42] A. Aranyi,[43] G. Bencze,[43] L. Boldizsar,[43] G. Debreczeni,[43] C. Hajdu,[43,b] D. Horvath,[43,l] A. Kapusi,[43] K. Krajczar,[43,m] A. Laszlo,[43] F. Sikler,[43] G. Vesztergombi,[43,m] N. Beni,[44] J. Molnar,[44] J. Palinkas,[44] Z. Szillasi,[44] V. Veszpremi,[44] P. Raics,[45] Z. L. Trocsanyi,[45] B. Ujvari,[45] S. Bansal,[46] S. B. Beri,[46] V. Bhatnagar,[46] N. Dhingra,[46] M. Jindal,[46] M. Kaur,[46] J. M. Kohli,[46] M. Z. Mehta,[46] N. Nishu,[46] L. K. Saini,[46] A. Sharma,[46] A. P. Singh,[46] J. B. Singh,[46] S. P. Singh,[46] S. Ahuja,[47] S. Bhattacharya,[47] B. C. Choudhary,[47] P. Gupta,[47] S. Jain,[47] S. Jain,[47] A. Kumar,[47] R. K. Shivpuri,[47] R. K. Choudhury,[48] D. Dutta,[48] S. Kailas,[48] S. K. Kataria,[48] A. K. Mohanty,[48,b] L. M. Pant,[48] P. Shukla,[48] P. Suggisetti,[48] T. Aziz,[49] M. Guchait,[49,n] A. Gurtu,[49] M. Maity,[49,o] D. Majumder,[49] G. Majumder,[49] K. Mazumdar,[49] G. B. Mohanty,[49] A. Saha,[49] K. Sudhakar,[49] N. Wickramage,[49] S. Banerjee,[50] S. Dugad,[50] N. K. Mondal,[50] H. Arfaei,[51] H. Bakhshiansohi,[51] S. M. Etesami,[51] A. Fahim,[51] M. Hashemi,[51] A. Jafari,[51] M. Khakzad,[51] A. Mohammadi,[51] M. Mohammadi Najafabadi,[51] S. Paktinat Mehdiabadi,[51] B. Safarzadeh,[51] M. Zeinali,[51] M. Abbrescia,[52a,52b] L. Barbone,[52a,52b] C. Calabria,[52a,52b] A. Colaleo,[52a] D. Creanza,[52a,52c] N. De Filippis,[52a,52c] M. De Palma,[52a,52b] A. Dimitrov,[52a] L. Fiore,[52a] G. Iaselli,[52a,52c] L. Lusito,[52a,52b,b] G. Maggi,[52a,52c] M. Maggi,[52a] N. Manna,[52a,52b] B. Marangelli,[52a,52b] S. My,[52a,52c] S. Nuzzo,[52a,52b] N. Pacifico,[52a,52b] G. A. Pierro,[52a] A. Pompili,[52a,52b] G. Pugliese,[52a,52c] F. Romano,[52a,52c] G. Roselli,[52a,52b] G. Selvaggi,[52a,52b] L. Silvestris,[52a] R. Trentadue,[52a] S. Tupputi,[52a,52b] G. Zito,[52a] G. Abbiendi,[53a] A. C. Benvenuti,[53a] D. Bonacorsi,[53a] S. Braibant-Giacomelli,[53a,53b] P. Capiluppi,[53a,53b] A. Castro,[53a,53b] F. R. Cavallo,[53a] M. Cuffiani,[53a,53b] G. M. Dallavalle,[53a] F. Fabbri,[53a] A. Fanfani,[53a,53b] D. Fasanella,[53a] P. Giacomelli,[53a] M. Giunta,[53a] C. Grandi,[53a] S. Marcellini,[53a] M. Meneghelli,[53a,53b] A. Montanari,[53a] F. L. Navarria,[53a,53b] F. Odorici,[53a] A. Perrotta,[53a] F. Primavera,[53a] A. M. Rossi,[53a,53b] T. Rovelli,[53a,53b] G. Siroli,[53a,53b] R. Travaglini,[53a,53b] S. Albergo,[54a,54b] G. Cappello,[54a,54b] M. Chiorboli,[54a,54b,b] S. Costa,[54a,54b] A. Tricomi,[54a,54b] C. Tuve,[54a] G. Barbagli,[55a] V. Ciulli,[55a,55b] C. Civinini,[55a] R. D'Alessandro,[55a,55b] E. Focardi,[55a,55b] S. Frosali,[55a,55b] E. Gallo,[55a] C. Genta,[55a] P. Lenzi,[55a,55b] M. Meschini,[55a] S. Paoletti,[55a] G. Sguazzoni,[55a] A. Tropiano,[55a,b] L. Benussi,[56] S. Bianco,[56]

S. Colafranceschi,[56,p] F. Fabbri,[56] D. Piccolo,[56] P. Fabbricatore,[57] R. Musenich,[57] A. Benaglia,[58a,58b] F. De Guio,[58a,58b,b] L. Di Matteo,[58a,58b] A. Ghezzi,[58a,58b,b] M. Malberti,[58a,58b] S. Malvezzi,[58a] A. Martelli,[58a,58b] A. Massironi,[58a,58b] D. Menasce,[58a] L. Moroni,[58a] M. Paganoni,[58a,58b] D. Pedrini,[58a] S. Ragazzi,[58a,58b] N. Redaelli,[58a] S. Sala,[58a] T. Tabarelli de Fatis,[58a,58b] V. Tancini,[58a,58b] S. Buontempo,[59a] C. A. Carrillo Montoya,[59a] A. Cimmino,[59a,59b] A. De Cosa,[59a,59b] M. De Gruttola,[59a,59b] F. Fabozzi,[59a,q] A. O. M. Iorio,[59a] L. Lista,[59a] M. Merola,[59a,59b] P. Noli,[59a,59b] P. Paolucci,[59a] P. Azzi,[60a] N. Bacchetta,[60a] P. Bellan,[60a,60b] D. Bisello,[60a,60b] A. Branca,[60a] R. Carlin,[60a,60b] P. Checchia,[60a] M. De Mattia,[60a,60b] T. Dorigo,[60a] U. Dosselli,[60a] F. Fanzago,[60a] F. Gasparini,[60a,60b] U. Gasparini,[60a,60b] P. Giubilato,[60a,60b] A. Gresele,[60a,60c] S. Lacaprara,[60a] I. Lazzizzera,[60a,60c] M. Margoni,[60a,60b] M. Mazzucato,[60a] A. T. Meneguzzo,[60a,60b] M. Nespolo,[60a] L. Perrozzi,[60a,b] N. Pozzobon,[60a,60b] P. Ronchese,[60a,60b] F. Simonetto,[60a,60b] E. Torassa,[60a] M. Tosi,[60a,60b] S. Vanini,[60a,60b] P. Zotto,[60a,60b] G. Zumerle,[60a,60b] P. Baesso,[61a,61b] U. Berzano,[61a] C. Riccardi,[61a,61b] P. Torre,[61a,61b] P. Vitulo,[61a,61b] C. Viviani,[61a,61b] M. Biasini,[62a,62b] G. M. Bilei,[62a] B. Caponeri,[62a,62b] L. Fanò,[62a,62b] P. Lariccia,[62a,62b] A. Lucaroni,[62a,62b,b] G. Mantovani,[62a,62b] M. Menichelli,[62a] A. Nappi,[62a,62b] A. Santocchia,[62a,62b] L. Servoli,[62a] S. Taroni,[62a,62b] M. Valdata,[62a,62b] R. Volpe,[62a,62b,b] P. Azzurri,[63a,63c] G. Bagliesi,[63a] J. Bernardini,[63a,63b] T. Boccali,[63a,b] G. Broccolo,[63a,63c] R. Castaldi,[63a] R. T. D'Agnolo,[63a,63c] R. Dell'Orso,[63a] F. Fiori,[63a,63b] L. Foà,[63a,63c] A. Giassi,[63a] A. Kraan,[63a] F. Ligabue,[63a,63c] T. Lomtadze,[63a] L. Martini,[63a] A. Messineo,[63a,63b] F. Palla,[63a] F. Palmonari,[63a] S. Sarkar,[63a,63c] A. T. Serban,[63a] P. Spagnolo,[63a] R. Tenchini,[63a] G. Tonelli,[63a,63b,b] A. Venturi,[63a,b] P. G. Verdini,[63a] L. Barone,[64a,64b] F. Cavallari,[64a] D. Del Re,[64a,64b] E. Di Marco,[64a,64b] M. Diemoz,[64a] D. Franci,[64a,64b] M. Grassi,[64a] E. Longo,[64a,64b] G. Organtini,[64a,64b] A. Palma,[64a,64b] F. Pandolfi,[64a,64b,b] R. Paramatti,[64a] S. Rahatlou,[64a,64b] N. Amapane,[65a,65b] R. Arcidiacono,[65a,65c] S. Argiro,[65a,65b] M. Arneodo,[65a,65c] C. Biino,[65a] C. Botta,[65a,65b,b] N. Cartiglia,[65a] R. Castello,[65a,65b] M. Costa,[65a,65b] N. Demaria,[65a] A. Graziano,[65a,65b,b] C. Mariotti,[65a] M. Marone,[65a,65b] S. Maselli,[65a] E. Migliore,[65a,65b] G. Mila,[65a,65b] V. Monaco,[65a,65b] M. Musich,[65a,65b] M. M. Obertino,[65a,65c] N. Pastrone,[65a] M. Pelliccioni,[65a,65b,b] A. Romero,[65a,65b] M. Ruspa,[65a,65c] R. Sacchi,[65a,65b] V. Sola,[65a,65b] A. Solano,[65a,65b] A. Staiano,[65a] D. Trocino,[65a,65b] A. Vilela Pereira,[65a,65b,b] F. Ambroglini,[66a,66b] S. Belforte,[66a] F. Cossutti,[66a] G. Della Ricca,[66a,66b] B. Gobbo,[66a] D. Montanino,[66a,66b] A. Penzo,[66a] S. G. Heo,[67] S. Chang,[68] J. Chung,[68] D. H. Kim,[68] G. N. Kim,[68] J. E. Kim,[68] D. J. Kong,[68] H. Park,[68] D. Son,[68] D. C. Son,[68] Zero Kim,[69] J. Y. Kim,[69] S. Song,[69] S. Choi,[70] B. Hong,[70] M. Jo,[70] H. Kim,[70] J. H. Kim,[70] T. J. Kim,[70] K. S. Lee,[70] D. H. Moon,[70] S. K. Park,[70] H. B. Rhee,[70] E. Seo,[70] S. Shin,[70] K. S. Sim,[70] M. Choi,[71] S. Kang,[71] H. Kim,[71] C. Park,[71] I. C. Park,[71] S. Park,[71] G. Ryu,[71] Y. Choi,[72] Y. K. Choi,[72] J. Goh,[72] J. Lee,[72] S. Lee,[72] H. Seo,[72] I. Yu,[72] M. J. Bilinskas,[73] I. Grigelionis,[73] M. Janulis,[73] D. Martisiute,[73] P. Petrov,[73] T. Sabonis,[73] H. Castilla Valdez,[74] E. De La Cruz Burelo,[74] R. Lopez-Fernandez,[74] A. Sánchez Hernández,[74] L. M. Villasenor-Cendejas,[74] S. Carrillo Moreno,[75] F. Vazquez Valencia,[75] H. A. Salazar Ibarguen,[76] E. Casimiro Linares,[77] A. Morelos Pineda,[77] M. A. Reyes-Santos,[77] P. Allfrey,[78] D. Krofcheck,[78] P. H. Butler,[79] R. Doesburg,[79] H. Silverwood,[79] M. Ahmad,[80] I. Ahmed,[80] M. I. Asghar,[80] H. R. Hoorani,[80] W. A. Khan,[80] T. Khurshid,[80] S. Qazi,[80] M. Cwiok,[81] W. Dominik,[81] K. Doroba,[81] A. Kalinowski,[81] M. Konecki,[81] J. Krolikowski,[81] T. Frueboes,[82] R. Gokieli,[82] M. Górski,[82] M. Kazana,[82] K. Nawrocki,[82] K. Romanowska-Rybinska,[82] M. Szleper,[82] G. Wrochna,[82] P. Zalewski,[82] N. Almeida,[83] A. David,[83] P. Faccioli,[83] P. G. Ferreira Parracho,[83] M. Gallinaro,[83] P. Martins,[83] P. Musella,[83] A. Nayak,[83] P. Q. Ribeiro,[83] J. Seixas,[83] P. Silva,[83] J. Varela,[83,b] H. K. Wöhri,[83] I. Belotelov,[84] P. Bunin,[84] M. Finger,[84] M. Finger, Jr.,[84] I. Golutvin,[84] A. Kamenev,[84] V. Karjavin,[84] G. Kozlov,[84] A. Lanev,[84] P. Moisenz,[84] V. Palichik,[84] V. Perelygin,[84] S. Shmatov,[84] V. Smirnov,[84] A. Volodko,[84] A. Zarubin,[84] N. Bondar,[85] V. Golovtsov,[85] Y. Ivanov,[85] V. Kim,[85] P. Levchenko,[85] V. Murzin,[85] V. Oreshkin,[85] I. Smirnov,[85] V. Sulimov,[85] L. Uvarov,[85] S. Vavilov,[85] A. Vorobyev,[85] Yu. Andreev,[86] S. Gninenko,[86] N. Golubev,[86] M. Kirsanov,[86] N. Krasnikov,[86] V. Matveev,[86] A. Pashenkov,[86] A. Toropin,[86] S. Troitsky,[86] V. Epshteyn,[87] V. Gavrilov,[87] V. Kaftanov,[87,a] M. Kossov,[87,b] A. Krokhotin,[87] N. Lychkovskaya,[87] G. Safronov,[87] S. Semenov,[87] V. Stolin,[87] E. Vlasov,[87] A. Zhokin,[87] E. Boos,[88] M. Dubinin,[88,r] L. Dudko,[88] A. Ershov,[88] A. Gribushin,[88] O. Kodolova,[88] I. Lokhtin,[88] S. Obraztsov,[88] S. Petrushanko,[88] L. Sarycheva,[88] V. Savrin,[88] A. Snigirev,[88] V. Andreev,[89] M. Azarkin,[89] I. Dremin,[89] M. Kirakosyan,[89] S. V. Rusakov,[89] A. Vinogradov,[89] I. Azhgirey,[90] S. Bitioukov,[90] V. Grishin,[90,b] V. Kachanov,[90] D. Konstantinov,[90] A. Korablev,[90] V. Krychkine,[90] V. Petrov,[90] R. Ryutin,[90] S. Slabospitsky,[90] A. Sobol,[90] L. Tourtchanovitch,[90] S. Troshin,[90] N. Tyurin,[90] A. Uzunian,[90] A. Volkov,[90] P. Adzic,[91,s] M. Djordjevic,[91] D. Krpic,[91,s] J. Milosevic,[91] M. Aguilar-Benitez,[92] J. Alcaraz Maestre,[92] P. Arce,[92] C. Battilana,[92] E. Calvo,[92] M. Cepeda,[92] M. Cerrada,[92] N. Colino,[92] B. De La Cruz,[92] C. Diez Pardos,[92] D. Domínguez Vázquez,[92]

C. Fernandez Bedoya,[92] J. P. Fernández Ramos,[92] A. Ferrando,[92] J. Flix,[92] M. C. Fouz,[92] P. Garcia-Abia,[92] O. Gonzalez Lopez,[92] S. Goy Lopez,[92] J. M. Hernandez,[92] M. I. Josa,[92] G. Merino,[92] J. Puerta Pelayo,[92] I. Redondo,[92] L. Romero,[92] J. Santaolalla,[92] C. Willmott,[92] C. Albajar,[93] G. Codispoti,[93] J. F. de Trocóniz,[93] J. Cuevas,[94] J. Fernandez Menendez,[94] S. Folgueras,[94] I. Gonzalez Caballero,[94] L. Lloret Iglesias,[94] J. M. Vizan Garcia,[94] J. A. Brochero Cifuentes,[95] I. J. Cabrillo,[95] A. Calderon,[95] M. Chamizo Llatas,[95] S. H. Chuang,[95] J. Duarte Campderros,[95] M. Felcini,[95,t] M. Fernandez,[95] G. Gomez,[95] J. Gonzalez Sanchez,[95] C. Jorda,[95] P. Lobelle Pardo,[95] A. Lopez Virto,[95] J. Marco,[95] R. Marco,[95] C. Martinez Rivero,[95] F. Matorras,[95] F. J. Munoz Sanchez,[95] J. Piedra Gomez,[95,u] T. Rodrigo,[95] A. Ruiz Jimeno,[95] L. Scodellaro,[95] M. Sobron Sanudo,[95] I. Vila,[95] R. Vilar Cortabitarte,[95] D. Abbaneo,[96] E. Auffray,[96] G. Auzinger,[96] P. Baillon,[96] A. H. Ball,[96] D. Barney,[96] A. J. Bell,[96,v] D. Benedetti,[96] C. Bernet,[96,d] W. Bialas,[96] P. Bloch,[96] A. Bocci,[96] S. Bolognesi,[96] H. Breuker,[96] G. Brona,[96] K. Bunkowski,[96] T. Camporesi,[96] E. Cano,[96] G. Cerminara,[96] T. Christiansen,[96] J. A. Coarasa Perez,[96] B. Curé,[96] D. D'Enterria,[96] A. De Roeck,[96] F. Duarte Ramos,[96] A. Elliott-Peisert,[96] B. Frisch,[96] W. Funk,[96] A. Gaddi,[96] S. Gennai,[96] G. Georgiou,[96] H. Gerwig,[96] D. Gigi,[96] K. Gill,[96] D. Giordano,[96] F. Glege,[96] R. Gomez-Reino Garrido,[96] M. Gouzevitch,[96] P. Govoni,[96] S. Gowdy,[96] L. Guiducci,[96] M. Hansen,[96] J. Harvey,[96] J. Hegeman,[96] B. Hegner,[96] C. Henderson,[96] G. Hesketh,[96] H. F. Hoffmann,[96] A. Honma,[96] V. Innocente,[96] P. Janot,[96] E. Karavakis,[96] P. Lecoq,[96] C. Leonidopoulos,[96] C. Lourenço,[96] A. Macpherson,[96] T. Mäki,[96] L. Malgeri,[96] M. Mannelli,[96] L. Masetti,[96] F. Meijers,[96] S. Mersi,[96] E. Meschi,[96] R. Moser,[96] M. U. Mozer,[96] M. Mulders,[96] E. Nesvold,[96,b] M. Nguyen,[96] T. Orimoto,[96] L. Orsini,[96] E. Perez,[96] A. Petrilli,[96] A. Pfeiffer,[96] M. Pierini,[96] M. Pimiä,[96] G. Polese,[96] A. Racz,[96] G. Rolandi,[96,w] T. Rommerskirchen,[96] C. Rovelli,[96,x] M. Rovere,[96] H. Sakulin,[96] C. Schäfer,[96] C. Schwick,[96] I. Segoni,[96] A. Sharma,[96] P. Siegrist,[96] M. Simon,[96] P. Sphicas,[96,y] D. Spiga,[96] M. Spiropulu,[96,r] F. Stöckli,[96] M. Stoye,[96] P. Tropea,[96] A. Tsirou,[96] A. Tsyganov,[96] G. I. Veres,[96,m] P. Vichoudis,[96] M. Voutilainen,[96] W. D. Zeuner,[96] W. Bertl,[97] K. Deiters,[97] W. Erdmann,[97] K. Gabathuler,[97] R. Horisberger,[97] Q. Ingram,[97] H. C. Kaestli,[97] S. König,[97] D. Kotlinski,[97] U. Langenegger,[97] F. Meier,[97] D. Renker,[97] T. Rohe,[97] J. Sibille,[97,z] A. Starodumov,[97,aa] P. Bortignon,[98] L. Caminada,[98,bb] Z. Chen,[98] S. Cittolin,[98] G. Dissertori,[98] M. Dittmar,[98] J. Eugster,[98] K. Freudenreich,[98] C. Grab,[98] A. Hervé,[98] W. Hintz,[98] P. Lecomte,[98] W. Lustermann,[98] C. Marchica,[98,bb] P. Martinez Ruiz del Arbol,[98] P. Meridiani,[98] P. Milenovic,[98,cc] F. Moortgat,[98] P. Nef,[98] F. Nessi-Tedaldi,[98] L. Pape,[98] F. Pauss,[98] T. Punz,[98] A. Rizzi,[98] F. J. Ronga,[98] M. Rossini,[98] L. Sala,[98] A. K. Sanchez,[98] M.-C. Sawley,[98] B. Stieger,[98] L. Tauscher,[98,a] A. Thea,[98] K. Theofilatos,[98] D. Treille,[98] C. Urscheler,[98] R. Wallny,[98,t] M. Weber,[98] L. Wehrli,[98] J. Weng,[98] E. Aguiló,[99] C. Amsler,[99] V. Chiochia,[99] S. De Visscher,[99] C. Favaro,[99] M. Ivova Rikova,[99] B. Millan Mejias,[99] C. Regenfus,[99] P. Robmann,[99] A. Schmidt,[99] H. Snoek,[99] L. Wilke,[99] Y. H. Chang,[100] K. H. Chen,[100] W. T. Chen,[100] S. Dutta,[100] A. Go,[100] C. M. Kuo,[100] S. W. Li,[100] W. Lin,[100] M. H. Liu,[100] Z. K. Liu,[100] Y. J. Lu,[100] J. H. Wu,[100] S. S. Yu,[100] P. Bartalini,[101] P. Chang,[101] Y. H. Chang,[101] Y. W. Chang,[101] Y. Chao,[101] K. F. Chen,[101] W.-S. Hou,[101] Y. Hsiung,[101] K. Y. Kao,[101] Y. J. Lei,[101] R.-S. Lu,[101] J. G. Shiu,[101] Y. M. Tzeng,[101] M. Wang,[101] A. Adiguzel,[102] M. N. Bakirci,[102,dd] S. Cerci,[102,ee] C. Dozen,[102] I. Dumanoglu,[102] E. Eskut,[102] S. Girgis,[102] G. Gokbulut,[102] Y. Guler,[102] E. Gurpinar,[102] I. Hos,[102] E. E. Kangal,[102] T. Karaman,[102] A. Kayis Topaksu,[102] A. Nart,[102] G. Onengut,[102] K. Ozdemir,[102] S. Ozturk,[102] A. Polatoz,[102] K. Sogut,[102,ff] B. Tali,[102] H. Topakli,[102,dd] D. Uzun,[102] L. N. Vergili,[102] M. Vergili,[102] C. Zorbilmez,[102] I. V. Akin,[103] T. Aliev,[103] S. Bilmis,[103] M. Deniz,[103] H. Gamsizkan,[103] A. M. Guler,[103] K. Ocalan,[103] A. Ozpineci,[103] M. Serin,[103] R. Sever,[103] U. E. Surat,[103] E. Yildirim,[103] M. Zeyrek,[103] M. Deliomeroglu,[104] D. Demir,[104,gg] E. Gülmez,[104] A. Halu,[104] B. Isildak,[104] M. Kaya,[104,hh] O. Kaya,[104,hh] S. Ozkorucuklu,[104,ii] N. Sonmez,[104,jj] L. Levchuk,[105] P. Bell,[106] F. Bostock,[106] J. J. Brooke,[106] T. L. Cheng,[106] E. Clement,[106] D. Cussans,[106] R. Frazier,[106] J. Goldstein,[106] M. Grimes,[106] M. Hansen,[106] D. Hartley,[106] G. P. Heath,[106] H. F. Heath,[106] B. Huckvale,[106] J. Jackson,[106] L. Kreczko,[106] S. Metson,[106] D. M. Newbold,[106,kk] K. Nirunpong,[106] A. Poll,[106] S. Senkin,[106] V. J. Smith,[106] S. Ward,[106] L. Basso,[107,ll] K. W. Bell,[107] A. Belyaev,[107,ll] C. Brew,[107] R. M. Brown,[107] B. Camanzi,[107] D. J. A. Cockerill,[107] J. A. Coughlan,[107] K. Harder,[107] S. Harper,[107] B. W. Kennedy,[107] E. Olaiya,[107] D. Petyt,[107] B. C. Radburn-Smith,[107] C. H. Shepherd-Themistocleous,[107] I. R. Tomalin,[107] W. J. Womersley,[107] S. D. Worm,[107] R. Bainbridge,[108] G. Ball,[108] J. Ballin,[108] R. Beuselinck,[108] O. Buchmuller,[108] D. Colling,[108] N. Cripps,[108] M. Cutajar,[108] G. Davies,[108] M. Della Negra,[108] J. Fulcher,[108] D. Futyan,[108] A. Guneratne Bryer,[108] G. Hall,[108] Z. Hatherell,[108] J. Hays,[108] G. Iles,[108] G. Karapostoli,[108] L. Lyons,[108] A.-M. Magnan,[108] J. Marrouche,[108] R. Nandi,[108] J. Nash,[108] A. Nikitenko,[108,aa] A. Papageorgiou,[108] M. Pesaresi,[108] K. Petridis,[108] M. Pioppi,[108,mm] D. M. Raymond,[108] N. Rompotis,[108] A. Rose,[108] M. J. Ryan,[108]

C. Seez,[108] P. Sharp,[108] A. Sparrow,[108] A. Tapper,[108] S. Tourneur,[108] M. Vazquez Acosta,[108] T. Virdee,[108] S. Wakefield,[108] D. Wardrope,[108] T. Whyntie,[108] M. Barrett,[109] M. Chadwick,[109] J. E. Cole,[109] P. R. Hobson,[109] A. Khan,[109] P. Kyberd,[109] D. Leslie,[109] W. Martin,[109] I. D. Reid,[109] L. Teodorescu,[109] K. Hatakeyama,[110] T. Bose,[111] E. Carrera Jarrin,[111] A. Clough,[111] C. Fantasia,[111] A. Heister,[111] J. St. John,[111] P. Lawson,[111] D. Lazic,[111] J. Rohlf,[111] D. Sperka,[111] L. Sulak,[111] A. Avetisyan,[112] S. Bhattacharya,[112] J. P. Chou,[112] D. Cutts,[112] A. Ferapontov,[112] U. Heintz,[112] S. Jabeen,[112] G. Kukartsev,[112] G. Landsberg,[112] M. Narain,[112] D. Nguyen,[112] M. Segala,[112] T. Speer,[112] K. V. Tsang,[112] M. A. Borgia,[113] R. Breedon,[113] M. Calderon De La Barca Sanchez,[113] D. Cebra,[113] S. Chauhan,[113] M. Chertok,[113] J. Conway,[113] P. T. Cox,[113] J. Dolen,[113] R. Erbacher,[113] E. Friis,[113] W. Ko,[113] A. Kopecky,[113] R. Lander,[113] H. Liu,[113] S. Maruyama,[113] T. Miceli,[113] M. Nikolic,[113] D. Pellett,[113] J. Robles,[113] S. Salur,[113] T. Schwarz,[113] M. Searle,[113] J. Smith,[113] M. Squires,[113] M. Tripathi,[113] R. Vasquez Sierra,[113] C. Veelken,[113] V. Andreev,[114] K. Arisaka,[114] D. Cline,[114] R. Cousins,[114] A. Deisher,[114] J. Duris,[114] S. Erhan,[114] C. Farrell,[114] J. Hauser,[114] M. Ignatenko,[114] C. Jarvis,[114] C. Plager,[114] G. Rakness,[114] P. Schlein,[114,a] J. Tucker,[114] V. Valuev,[114] J. Babb,[115] R. Clare,[115] J. Ellison,[115] J. W. Gary,[115] F. Giordano,[115] G. Hanson,[115] G. Y. Jeng,[115] S. C. Kao,[115] F. Liu,[115] H. Liu,[115] A. Luthra,[115] H. Nguyen,[115] G. Pasztor,[115,nn] A. Satpathy,[115] B. C. Shen,[115,a] R. Stringer,[115] J. Sturdy,[115] S. Sumowidagdo,[115] R. Wilken,[115] S. Wimpenny,[115] W. Andrews,[116] J. G. Branson,[116] G. B. Cerati,[116] E. Dusinberre,[116] D. Evans,[116] F. Golf,[116] A. Holzner,[116] R. Kelley,[116] M. Lebourgeois,[116] J. Letts,[116] B. Mangano,[116] J. Muelmenstaedt,[116] S. Padhi,[116] C. Palmer,[116] G. Petrucciani,[116] H. Pi,[116] M. Pieri,[116] R. Ranieri,[116] M. Sani,[116] V. Sharma,[116,b] S. Simon,[116] Y. Tu,[116] A. Vartak,[116] F. Würthwein,[116] A. Yagil,[116] D. Barge,[117] R. Bellan,[117] C. Campagnari,[117] M. D'Alfonso,[117] T. Danielson,[117] K. Flowers,[117] P. Geffert,[117] J. Incandela,[117] C. Justus,[117] P. Kalavase,[117] S. A. Koay,[117] D. Kovalskyi,[117] V. Krutelyov,[117] S. Lowette,[117] N. Mccoll,[117] V. Pavlunin,[117] F. Rebassoo,[117] J. Ribnik,[117] J. Richman,[117] R. Rossin,[117] D. Stuart,[117] W. To,[117] J. R. Vlimant,[117] A. Bornheim,[118] J. Bunn,[118] Y. Chen,[118] M. Gataullin,[118] D. Kcira,[118] V. Litvine,[118] Y. Ma,[118] A. Mott,[118] H. B. Newman,[118] C. Rogan,[118] V. Timciuc,[118] P. Traczyk,[118] J. Veverka,[118] R. Wilkinson,[118] Y. Yang,[118] R. Y. Zhu,[118] B. Akgun,[119] R. Carroll,[119] T. Ferguson,[119] Y. Iiyama,[119] D. W. Jang,[119] S. Y. Jun,[119] Y. F. Liu,[119] M. Paulini,[119] J. Russ,[119] N. Terentyev,[119] H. Vogel,[119] I. Vorobiev,[119] J. P. Cumalat,[120] M. E. Dinardo,[120] B. R. Drell,[120] C. J. Edelmaier,[120] W. T. Ford,[120] B. Heyburn,[120] E. Luiggi Lopez,[120] U. Nauenberg,[120] J. G. Smith,[120] K. Stenson,[120] K. A. Ulmer,[120] S. R. Wagner,[120] S. L. Zang,[120] L. Agostino,[121] J. Alexander,[121] A. Chatterjee,[121] S. Das,[121] N. Eggert,[121] L. J. Fields,[121] L. K. Gibbons,[121] B. Heltsley,[121] W. Hopkins,[121] A. Khukhunaishvili,[121] B. Kreis,[121] V. Kuznetsov,[121] G. Nicolas Kaufman,[121] J. R. Patterson,[121] D. Puigh,[121] D. Riley,[121] A. Ryd,[121] X. Shi,[121] W. Sun,[121] W. D. Teo,[121] J. Thom,[121] J. Thompson,[121] J. Vaughan,[121] Y. Weng,[121] L. Winstrom,[121] P. Wittich,[121] A. Biselli,[122] G. Cirino,[122] D. Winn,[122] S. Abdullin,[123] M. Albrow,[123] J. Anderson,[123] G. Apollinari,[123] M. Atac,[123] J. A. Bakken,[123] S. Banerjee,[123] L. A. T. Bauerdick,[123] A. Beretvas,[123] J. Berryhill,[123] P. C. Bhat,[123] I. Bloch,[123] F. Borcherding,[123] K. Burkett,[123] J. N. Butler,[123] V. Chetluru,[123] H. W. K. Cheung,[123] F. Chlebana,[123] S. Cihangir,[123] M. Demarteau,[123] D. P. Eartly,[123] V. D. Elvira,[123] S. Esen,[123] I. Fisk,[123] J. Freeman,[123] Y. Gao,[123] E. Gottschalk,[123] D. Green,[123] K. Gunthoti,[123] O. Gutsche,[123] A. Hahn,[123] J. Hanlon,[123] R. M. Harris,[123] J. Hirschauer,[123] B. Hooberman,[123] E. James,[123] H. Jensen,[123] M. Johnson,[123] U. Joshi,[123] R. Khatiwada,[123] B. Kilminster,[123] B. Klima,[123] K. Kousouris,[123] S. Kunori,[123] S. Kwan,[123] P. Limon,[123] R. Lipton,[123] J. Lykken,[123] K. Maeshima,[123] J. M. Marraffino,[123] D. Mason,[123] P. McBride,[123] T. McCauley,[123] T. Miao,[123] K. Mishra,[123] S. Mrenna,[123] Y. Musienko,[123,oo] C. Newman-Holmes,[123] V. O'Dell,[123] S. Popescu,[123,pp] R. Pordes,[123] O. Prokofyev,[123] N. Saoulidou,[123] E. Sexton-Kennedy,[123] S. Sharma,[123] A. Soha,[123] W. J. Spalding,[123] L. Spiegel,[123] P. Tan,[123] L. Taylor,[123] S. Tkaczyk,[123] L. Uplegger,[123] E. W. Vaandering,[123] R. Vidal,[123] J. Whitmore,[123] W. Wu,[123] F. Yang,[123] F. Yumiceva,[123] J. C. Yun,[123] D. Acosta,[124] P. Avery,[124] D. Bourilkov,[124] M. Chen,[124] G. P. Di Giovanni,[124] D. Dobur,[124] A. Drozdetskiy,[124] R. D. Field,[124] M. Fisher,[124] Y. Fu,[124] I. K. Furic,[124] J. Gartner,[124] S. Goldberg,[124] B. Kim,[124] S. Klimenko,[124] J. Konigsberg,[124] A. Korytov,[124] A. Kropivnitskaya,[124] T. Kypreos,[124] K. Matchev,[124] G. Mitselmakher,[124] L. Muniz,[124] Y. Pakhotin,[124] C. Prescott,[124] R. Remington,[124] M. Schmitt,[124] B. Scurlock,[124] P. Sellers,[124] N. Skhirtladze,[124] D. Wang,[124] J. Yelton,[124] M. Zakaria,[124] C. Ceron,[125] V. Gaultney,[125] L. Kramer,[125] L. M. Lebolo,[125] S. Linn,[125] P. Markowitz,[125] G. Martinez,[125] J. L. Rodriguez,[125] T. Adams,[126] A. Askew,[126] D. Bandurin,[126] J. Bochenek,[126] J. Chen,[126] B. Diamond,[126] S. V. Gleyzer,[126] J. Haas,[126] S. Hagopian,[126] V. Hagopian,[126] M. Jenkins,[126] K. F. Johnson,[126] H. Prosper,[126] S. Sekmen,[126] V. Veeraraghavan,[126] M. M. Baarmand,[127] B. Dorney,[127] S. Guragain,[127] M. Hohlmann,[127] H. Kalakhety,[127] R. Ralich,[127] I. Vodopiyanov,[127] M. R. Adams,[128] I. M. Anghel,[128] L. Apanasevich,[128] Y. Bai,[128] V. E. Bazterra,[128] R. R. Betts,[128]

J. Callner,[128] R. Cavanaugh,[128] C. Dragoiu,[128] E. J. Garcia-Solis,[128] C. E. Gerber,[128] D. J. Hofman,[128] S. Khalatyan,[128] F. Lacroix,[128] C. O'Brien,[128] C. Silvestre,[128] A. Smoron,[128] D. Strom,[128] N. Varelas,[128] U. Akgun,[129] E. A. Albayrak,[129] B. Bilki,[129] K. Cankocak,[129] W. Clarida,[129] F. Duru,[129] C. K. Lae,[129] E. McCliment,[129] J.-P. Merlo,[129] H. Mermerkaya,[129] A. Mestvirishvili,[129] A. Moeller,[129] J. Nachtman,[129] C. R. Newsom,[129] E. Norbeck,[129] J. Olson,[129] Y. Onel,[129] F. Ozok,[129] S. Sen,[129] J. Wetzel,[129] T. Yetkin,[129] K. Yi,[129] B. A. Barnett,[130] B. Blumenfeld,[130] A. Bonato,[130] C. Eskew,[130] D. Fehling,[130] G. Giurgiu,[130] A. V. Gritsan,[130] Z. J. Guo,[130] G. Hu,[130] P. Maksimovic,[130] S. Rappoccio,[130] M. Swartz,[130] N. V. Tran,[130] A. Whitbeck,[130] P. Baringer,[131] A. Bean,[131] G. Benelli,[131] O. Grachov,[131] M. Murray,[131] D. Noonan,[131] V. Radicci,[131] S. Sanders,[131] J. S. Wood,[131] V. Zhukova,[131] T. Bolton,[132] I. Chakaberia,[132] A. Ivanov,[132] M. Makouski,[132] Y. Maravin,[132] S. Shrestha,[132] I. Svintradze,[132] Z. Wan,[132] J. Gronberg,[133] D. Lange,[133] D. Wright,[133] A. Baden,[134] M. Boutemeur,[134] S. C. Eno,[134] D. Ferencek,[134] J. A. Gomez,[134] N. J. Hadley,[134] R. G. Kellogg,[134] M. Kirn,[134] Y. Lu,[134] A. C. Mignerey,[134] K. Rossato,[134] P. Rumerio,[134] F. Santanastasio,[134] A. Skuja,[134] J. Temple,[134] M. B. Tonjes,[134] S. C. Tonwar,[134] E. Twedt,[134] B. Alver,[135] G. Bauer,[135] J. Bendavid,[135] W. Busza,[135] E. Butz,[135] I. A. Cali,[135] M. Chan,[135] V. Dutta,[135] P. Everaerts,[135] G. Gomez Ceballos,[135] M. Goncharov,[135] K. A. Hahn,[135] P. Harris,[135] Y. Kim,[135] M. Klute,[135] Y.-J. Lee,[135] W. Li,[135] C. Loizides,[135] P. D. Luckey,[135] T. Ma,[135] S. Nahn,[135] C. Paus,[135] D. Ralph,[135] C. Roland,[135] G. Roland,[135] M. Rudolph,[135] G. S. F. Stephans,[135] K. Sumorok,[135] K. Sung,[135] E. A. Wenger,[135] S. Xie,[135] M. Yang,[135] Y. Yilmaz,[135] A. S. Yoon,[135] M. Zanetti,[135] P. Cole,[136] S. I. Cooper,[136] P. Cushman,[136] B. Dahmes,[136] A. De Benedetti,[136] P. R. Dudero,[136] G. Franzoni,[136] J. Haupt,[136] K. Klapoetke,[136] Y. Kubota,[136] J. Mans,[136] V. Rekovic,[136] R. Rusack,[136] M. Sasseville,[136] A. Singovsky,[136] L. M. Cremaldi,[137] R. Godang,[137] R. Kroeger,[137] L. Perera,[137] R. Rahmat,[137] D. A. Sanders,[137] D. Summers,[137] K. Bloom,[138] S. Bose,[138] J. Butt,[138] D. R. Claes,[138] A. Dominguez,[138] M. Eads,[138] J. Keller,[138] T. Kelly,[138] I. Kravchenko,[138] J. Lazo-Flores,[138] C. Lundstedt,[138] H. Malbouisson,[138] S. Malik,[138] G. R. Snow,[138] U. Baur,[139] A. Godshalk,[139] I. Iashvili,[139] A. Kharchilava,[139] A. Kumar,[139] S. P. Shipkowski,[139] K. Smith,[139] G. Alverson,[140] E. Barberis,[140] D. Baumgartel,[140] O. Boeriu,[140] M. Chasco,[140] K. Kaadze,[140] S. Reucroft,[140] J. Swain,[140] D. Wood,[140] J. Zhang,[140] A. Anastassov,[141] A. Kubik,[141] N. Odell,[141] R. A. Ofierzynski,[141] B. Pollack,[141] A. Pozdnyakov,[141] M. Schmitt,[141] S. Stoynev,[141] M. Velasco,[141] S. Won,[141] L. Antonelli,[142] D. Berry,[142] M. Hildreth,[142] C. Jessop,[142] D. J. Karmgard,[142] J. Kolb,[142] T. Kolberg,[142] K. Lannon,[142] W. Luo,[142] S. Lynch,[142] N. Marinelli,[142] D. M. Morse,[142] T. Pearson,[142] R. Ruchti,[142] J. Slaunwhite,[142] N. Valls,[142] J. Warchol,[142] M. Wayne,[142] J. Ziegler,[142] B. Bylsma,[143] L. S. Durkin,[143] J. Gu,[143] C. Hill,[143] P. Killewald,[143] K. Kotov,[143] T. Y. Ling,[143] M. Rodenburg,[143] G. Williams,[143] N. Adam,[144] E. Berry,[144] P. Elmer,[144] D. Gerbaudo,[144] V. Halyo,[144] P. Hebda,[144] A. Hunt,[144] J. Jones,[144] E. Laird,[144] D. Lopes Pegna,[144] D. Marlow,[144] T. Medvedeva,[144] M. Mooney,[144] J. Olsen,[144] P. Piroué,[144] X. Quan,[144] H. Saka,[144] D. Stickland,[144] C. Tully,[144] J. S. Werner,[144] A. Zuranski,[144] J. G. Acosta,[145] X. T. Huang,[145] A. Lopez,[145] H. Mendez,[145] S. Oliveros,[145] J. E. Ramirez Vargas,[145] A. Zatserklyaniy,[145] E. Alagoz,[146] V. E. Barnes,[146] G. Bolla,[146] L. Borrello,[146] D. Bortoletto,[146] A. Everett,[146] A. F. Garfinkel,[146] Z. Gecse,[146] L. Gutay,[146] Z. Hu,[146] M. Jones,[146] O. Koybasi,[146] A. T. Laasanen,[146] N. Leonardo,[146] C. Liu,[146] V. Maroussov,[146] P. Merkel,[146] D. H. Miller,[146] N. Neumeister,[146] K. Potamianos,[146] I. Shipsey,[146] D. Silvers,[146] A. Svyatkovskiy,[146] H. D. Yoo,[146] J. Zablocki,[146] Y. Zheng,[146] P. Jindal,[147] N. Parashar,[147] C. Boulahouache,[148] V. Cuplov,[148] K. M. Ecklund,[148] F. J. M. Geurts,[148] J. H. Liu,[148] J. Morales,[148] B. P. Padley,[148] R. Redjimi,[148] J. Roberts,[148] J. Zabel,[148] B. Betchart,[149] A. Bodek,[149] Y. S. Chung,[149] R. Covarelli,[149] P. de Barbaro,[149] R. Demina,[149] Y. Eshaq,[149] H. Flacher,[149] A. Garcia-Bellido,[149] P. Goldenzweig,[149] Y. Gotra,[149] J. Han,[149] A. Harel,[149] D. C. Miner,[149] D. Orbaker,[149] G. Petrillo,[149] D. Vishnevskiy,[149] M. Zielinski,[149] A. Bhatti,[150] L. Demortier,[150] K. Goulianos,[150] G. Lungu,[150] C. Mesropian,[150] M. Yan,[150] O. Atramentov,[151] A. Barker,[151] D. Duggan,[151] Y. Gershtein,[151] R. Gray,[151] E. Halkiadakis,[151] D. Hidas,[151] D. Hits,[151] A. Lath,[151] S. Panwalkar,[151] R. Patel,[151] A. Richards,[151] K. Rose,[151] S. Schnetzer,[151] S. Somalwar,[151] R. Stone,[151] S. Thomas,[151] G. Cerizza,[152] M. Hollingsworth,[152] S. Spanier,[152] Z. C. Yang,[152] A. York,[152] J. Asaadi,[153] R. Eusebi,[153] J. Gilmore,[153] A. Gurrola,[153] T. Kamon,[153] V. Khotilovich,[153] R. Montalvo,[153] C. N. Nguyen,[153] I. Osipenkov,[153] J. Pivarski,[153] A. Safonov,[153] S. Sengupta,[153] A. Tatarinov,[153] D. Toback,[153] M. Weinberger,[153] N. Akchurin,[154] C. Bardak,[154] J. Damgov,[154] C. Jeong,[154] K. Kovitanggoon,[154] S. W. Lee,[154] P. Mane,[154] Y. Roh,[154] A. Sill,[154] I. Volobouev,[154] R. Wigmans,[154] E. Yazgan,[154] E. Appelt,[155] E. Brownson,[155] D. Engh,[155] C. Florez,[155] W. Gabella,[155] W. Johns,[155] P. Kurt,[155] C. Maguire,[155] A. Melo,[155] P. Sheldon,[155] J. Velkovska,[155] M. W. Arenton,[156] M. Balazs,[156] S. Boutle,[156] M. Buehler,[156] S. Conetti,[156] B. Cox,[156] B. Francis,[156] R. Hirosky,[156] A. Ledovskoy,[156] C. Lin,[156] C. Neu,[156]

R. Yohay,[156] S. Gollapinni,[157] R. Harr,[157] P. E. Karchin,[157] P. Lamichhane,[157] M. Mattson,[157] C. Milstène,[157] A. Sakharov,[157] M. Anderson,[158] M. Bachtis,[158] J. N. Bellinger,[158] D. Carlsmith,[158] S. Dasu,[158] J. Efron,[158] L. Gray,[158] K. S. Grogg,[158] M. Grothe,[158] R. Hall-Wilton,[158,b] M. Herndon,[158] P. Klabbers,[158] J. Klukas,[158] A. Lanaro,[158] C. Lazaridis,[158] J. Leonard,[158] D. Lomidze,[158] R. Loveless,[158] A. Mohapatra,[158] D. Reeder,[158] I. Ross,[158] A. Savin,[158] W. H. Smith,[158] J. Swanson,[158] and M. Weinberg[158]

(CMS Collaboration)

[1]*Yerevan Physics Institute, Yerevan, Armenia*
[2]*Institut für Hochenergiephysik der OeAW, Wien, Austria*
[3]*National Centre for Particle and High Energy Physics, Minsk, Belarus*
[4]*Universiteit Antwerpen, Antwerpen, Belgium*
[5]*Vrije Universiteit Brussel, Brussel, Belgium*
[6]*Université Libre de Bruxelles, Bruxelles, Belgium*
[7]*Ghent University, Ghent, Belgium*
[8]*Université Catholique de Louvain, Louvain-la-Neuve, Belgium*
[9]*Université de Mons, Mons, Belgium*
[10]*Centro Brasileiro de Pesquisas Fisicas, Rio de Janeiro, Brazil*
[11]*Universidade do Estado do Rio de Janeiro, Rio de Janeiro, Brazil*
[12]*Instituto de Fisica Teorica, Universidade Estadual Paulista, Sao Paulo, Brazil*
[13]*Institute for Nuclear Research and Nuclear Energy, Sofia, Bulgaria*
[14]*University of Sofia, Sofia, Bulgaria*
[15]*Institute of High Energy Physics, Beijing, China*
[16]*State Key Laboratory of Nuclear Physics and Technology, Peking University, Beijing, China*
[17]*Universidad de Los Andes, Bogota, Colombia*
[18]*Technical University of Split, Split, Croatia*
[19]*University of Split, Split, Croatia*
[20]*Institute Rudjer Boskovic, Zagreb, Croatia*
[21]*University of Cyprus, Nicosia, Cyprus*
[22]*Academy of Scientific Research and Technology of the Arab Republic of Egypt, Egyptian Network of High Energy Physics, Cairo, Egypt*
[23]*National Institute of Chemical Physics and Biophysics, Tallinn, Estonia*
[24]*Department of Physics, University of Helsinki, Helsinki, Finland*
[25]*Helsinki Institute of Physics, Helsinki, Finland*
[26]*Lappeenranta University of Technology, Lappeenranta, Finland*
[27]*Laboratoire d'Annecy-le-Vieux de Physique des Particules, IN2P3-CNRS, Annecy-le-Vieux, France*
[28]*DSM/IRFU, CEA/Saclay, Gif-sur-Yvette, France*
[29]*Laboratoire Leprince-Ringuet, Ecole Polytechnique, IN2P3-CNRS, Palaiseau, France*
[30]*Institut Pluridisciplinaire Hubert Curien, Université de Strasbourg, Université de Haute Alsace Mulhouse, CNRS/IN2P3, Strasbourg, France*
[31]*Centre de Calcul de l'Institut National de Physique Nucleaire et de Physique des Particules (IN2P3), Villeurbanne, France*
[32]*Université de Lyon, Université Claude Bernard Lyon 1, CNRS-IN2P3, Institut de Physique Nucléaire de Lyon, Villeurbanne, France*
[33]*E. Andronikashvili Institute of Physics, Academy of Science, Tbilisi, Georgia*
[34]*RWTH Aachen University, I. Physikalisches Institut, Aachen, Germany*
[35]*RWTH Aachen University, III. Physikalisches Institut A, Aachen, Germany*
[36]*RWTH Aachen University, III. Physikalisches Institut B, Aachen, Germany*
[37]*Deutsches Elektronen-Synchrotron, Hamburg, Germany*
[38]*University of Hamburg, Hamburg, Germany*
[39]*Institut für Experimentelle Kernphysik, Karlsruhe, Germany*
[40]*Institute of Nuclear Physics Demokritos, Aghia Paraskevi, Greece*
[41]*University of Athens, Athens, Greece*
[42]*University of Ioánnina, Ioánnina, Greece*
[43]*KFKI Research Institute for Particle and Nuclear Physics, Budapest, Hungary*
[44]*Institute of Nuclear Research ATOMKI, Debrecen, Hungary*
[45]*University of Debrecen, Debrecen, Hungary*
[46]*Panjab University, Chandigarh, India*
[47]*University of Delhi, Delhi, India*
[48]*Bhabha Atomic Research Centre, Mumbai, India*
[49]*Tata Institute of Fundamental Research - EHEP, Mumbai, India*

[50]*Tata Institute of Fundamental Research - HECR, Mumbai, India*
[51]*Institute for Research and Fundamental Sciences (IPM), Tehran, Iran*
[52a]*INFN Sezione di Bari, Bari, Italy*
[52b]*Università di Bari, Bari, Italy*
[52c]*Politecnico di Bari, Bari, Italy*
[53a]*INFN Sezione di Bologna, Bologna, Italy*
[53b]*Università di Bologna, Bologna, Italy*
[54a]*INFN Sezione di Catania, Catania, Italy*
[54b]*Università di Catania, Catania, Italy*
[55a]*INFN Sezione di Firenze, Firenze, Italy*
[55b]*Università di Firenze, Firenze, Italy*
[56]*INFN Laboratori Nazionali di Frascati, Frascati, Italy*
[57]*INFN Sezione di Genova, Genova, Italy*
[58a]*INFN Sezione di Milano-Bicocca, Milano, Italy*
[58b]*Università di Milano-Bicocca, Milano, Italy*
[59a]*INFN Sezione di Napoli, Napoli, Italy*
[59b]*Università di Napoli "Federico II", Napoli, Italy*
[60a]*INFN Sezione di Padova, Padova, Italy*
[60b]*Università di Padova, Padova, Italy*
[60c]*Università di Trento (Trento), Padova, Italy*
[61a]*INFN Sezione di Pavia, Pavia, Italy*
[61b]*Università di Pavia, Pavia, Italy*
[62a]*INFN Sezione di Perugia, Perugia, Italy*
[62b]*Università di Perugia, Perugia, Italy*
[63a]*INFN Sezione di Pisa, Pisa, Italy*
[63b]*Università di Pisa, Pisa, Italy*
[63c]*Scuola Normale Superiore di Pisa, Pisa, Italy*
[64a]*INFN Sezione di Roma, Roma, Italy*
[64b]*Università di Roma La Sapienza, Roma, Italy*
[65a]*INFN Sezione di Torino, Torino, Italy*
[65b]*Università di Torino, Torino, Italy*
[65c]*Università del Piemonte Orientale (Novara)*
[66a]*INFN Sezione di Trieste, Trieste, Italy*
[66b]*Università di Trieste, Trieste, Italy*
[67]*Kangwon National University, Chunchon, Korea*
[68]*Kyungpook National University, Daegu, Korea*
[69]*Chonnam National University, Institute for Universe and Elementary Particles, Kwangju, Korea*
[70]*Korea University, Seoul, Korea*
[71]*University of Seoul, Seoul, Korea*
[72]*Sungkyunkwan University, Suwon, Korea*
[73]*Vilnius University, Vilnius, Lithuania*
[74]*Centro de Investigacion y de Estudios Avanzados del IPN, Mexico City, Mexico*
[75]*Universidad Iberoamericana, Mexico City, Mexico*
[76]*Benemerita Universidad Autonoma de Puebla, Puebla, Mexico*
[77]*Universidad Autónoma de San Luis Potosí, San Luis Potosí, Mexico*
[78]*University of Auckland, Auckland, New Zealand*
[79]*University of Canterbury, Christchurch, New Zealand*
[80]*National Centre for Physics, Quaid-I-Azam University, Islamabad, Pakistan*
[81]*Institute of Experimental Physics, Faculty of Physics, University of Warsaw, Warsaw, Poland*
[82]*Soltan Institute for Nuclear Studies, Warsaw, Poland*
[83]*Laboratório de Instrumentação e Física Experimental de Partículas, Lisboa, Portugal*
[84]*Joint Institute for Nuclear Research, Dubna, Russia*
[85]*Petersburg Nuclear Physics Institute, Gatchina (St Petersburg), Russia*
[86]*Institute for Nuclear Research, Moscow, Russia*
[87]*Institute for Theoretical and Experimental Physics, Moscow, Russia*
[88]*Moscow State University, Moscow, Russia*
[89]*P. N. Lebedev Physical Institute, Moscow, Russia*
[90]*State Research Center of Russian Federation, Institute for High Energy Physics, Protvino, Russia*
[91]*University of Belgrade, Faculty of Physics and Vinca Institute of Nuclear Sciences, Belgrade, Serbia*
[92]*Centro de Investigaciones Energéticas Medioambientales y Tecnológicas (CIEMAT), Madrid, Spain*
[93]*Universidad Autónoma de Madrid, Madrid, Spain*

[94]*Universidad de Oviedo, Oviedo, Spain*
[95]*Instituto de Física de Cantabria (IFCA), CSIC-Universidad de Cantabria, Santander, Spain*
[96]*CERN, European Organization for Nuclear Research, Geneva, Switzerland*
[97]*Paul Scherrer Institut, Villigen, Switzerland*
[98]*Institute for Particle Physics, ETH Zurich, Zurich, Switzerland*
[99]*Universität Zürich, Zurich, Switzerland*
[100]*National Central University, Chung-Li, Taiwan*
[101]*National Taiwan University (NTU), Taipei, Taiwan*
[102]*Cukurova University, Adana, Turkey*
[103]*Middle East Technical University, Physics Department, Ankara, Turkey*
[104]*Bogazici University, Istanbul, Turkey*
[105]*National Scientific Center, Kharkov Institute of Physics and Technology, Kharkov, Ukraine*
[106]*University of Bristol, Bristol, United Kingdom*
[107]*Rutherford Appleton Laboratory, Didcot, United Kingdom*
[108]*Imperial College, London, United Kingdom*
[109]*Brunel University, Uxbridge, United Kingdom*
[110]*Baylor University, Waco, USA*
[111]*Boston University, Boston, USA*
[112]*Brown University, Providence, USA*
[113]*University of California, Davis, Davis, USA*
[114]*University of California, Los Angeles, Los Angeles, USA*
[115]*University of California, Riverside, Riverside, USA*
[116]*University of California, San Diego, La Jolla, USA*
[117]*University of California, Santa Barbara, Santa Barbara, USA*
[118]*California Institute of Technology, Pasadena, USA*
[119]*Carnegie Mellon University, Pittsburgh, USA*
[120]*University of Colorado at Boulder, Boulder, USA*
[121]*Cornell University, Ithaca, USA*
[122]*Fairfield University, Fairfield, USA*
[123]*Fermi National Accelerator Laboratory, Batavia, USA*
[124]*University of Florida, Gainesville, USA*
[125]*Florida International University, Miami, USA*
[126]*Florida State University, Tallahassee, USA*
[127]*Florida Institute of Technology, Melbourne, USA*
[128]*University of Illinois at Chicago (UIC), Chicago, USA*
[129]*The University of Iowa, Iowa City, USA*
[130]*Johns Hopkins University, Baltimore, USA*
[131]*The University of Kansas, Lawrence, USA*
[132]*Kansas State University, Manhattan, USA*
[133]*Lawrence Livermore National Laboratory, Livermore, USA*
[134]*University of Maryland, College Park, USA*
[135]*Massachusetts Institute of Technology, Cambridge, USA*
[136]*University of Minnesota, Minneapolis, USA*
[137]*University of Mississippi, University, USA*
[138]*University of Nebraska-Lincoln, Lincoln, USA*
[139]*State University of New York at Buffalo, Buffalo, USA*
[140]*Northeastern University, Boston, USA*
[141]*Northwestern University, Evanston, USA*
[142]*University of Notre Dame, Notre Dame, USA*
[143]*The Ohio State University, Columbus, USA*
[144]*Princeton University, Princeton, USA*
[145]*University of Puerto Rico, Mayaguez, USA*
[146]*Purdue University, West Lafayette, USA*
[147]*Purdue University Calumet, Hammond, USA*
[148]*Rice University, Houston, USA*
[149]*University of Rochester, Rochester, USA*
[150]*The Rockefeller University, New York, USA*
[151]*Rutgers, the State University of New Jersey, Piscataway, USA*
[152]*University of Tennessee, Knoxville, USA*
[153]*Texas A&M University, College Station, USA*
[154]*Texas Tech University, Lubbock, USA*

[155]*Vanderbilt University, Nashville, USA*
[156]*University of Virginia, Charlottesville, USA*
[157]*Wayne State University, Detroit, USA*
[158]*University of Wisconsin, Madison, USA*

[a]Deceased.
[b]Also at CERN, European Organization for Nuclear Research, Geneva, Switzerland.
[c]Also at Universidade Federal do ABC, Santo Andre, Brazil.
[d]Also at Laboratoire Leprince-Ringuet, Ecole Polytechnique, IN2P3-CNRS, Palaiseau, France.
[e]Also at Suez Canal University, Suez, Egypt.
[f]Also at Fayoum University, El-Fayoum, Egypt.
[g]Also at Soltan Institute for Nuclear Studies, Warsaw, Poland.
[h]Also at Massachusetts Institute of Technology, Cambridge, USA.
[i]Also at Université de Haute-Alsace, Mulhouse, France.
[j]Also at Brandenburg University of Technology, Cottbus, Germany.
[k]Also at Moscow State University, Moscow, Russia.
[l]Also at Institute of Nuclear Research ATOMKI, Debrecen, Hungary.
[m]Also at Eötvös Loránd University, Budapest, Hungary.
[n]Also at Tata Institute of Fundamental Research - HECR, Mumbai, India.
[o]Also at University of Visva-Bharati, Santiniketan, India.
[p]Also at Facoltà Ingegneria Università di Roma La Sapienza, Roma, Italy.
[q]Also at Università della Basilicata, Potenza, Italy.
[r]Also at California Institute of Technology, Pasadena, USA.
[s]Also at Faculty of Physics of University of Belgrade, Belgrade, Serbia.
[t]Also at University of California, Los Angeles, Los Angeles, USA.
[u]Also at University of Florida, Gainesville, USA.
[v]Also at Université de Genève, Geneva, Switzerland.
[w]Also at Scuola Normale e Sezione dell' INFN, Pisa, Italy.
[x]Also at INFN Sezione di Roma, Università di Roma La Sapienza, Roma, Italy.
[y]Also at University of Athens, Athens, Greece.
[z]Also at The University of Kansas, Lawrence, USA.
[aa]Also at Institute for Theoretical and Experimental Physics, Moscow, Russia.
[bb]Also at Paul Scherrer Institut, Villigen, Switzerland.
[cc]Also at University of Belgrade, Faculty of Physics and Vinca Institute of Nuclear Sciences, Belgrade, Serbia.
[dd]Also at Gaziosmanpasa University, Tokat, Turkey.
[ee]Also at Adiyaman University, Adiyaman, Turkey.
[ff]Also at Mersin University, Mersin, Turkey.
[gg]Also at Izmir Institute of Technology, Izmir, Turkey.
[hh]Also at Kafkas University, Kars, Turkey.
[ii]Also at Suleyman Demirel University, Isparta, Turkey.
[jj]Also at Ege University, Izmir, Turkey.
[kk]Also at Rutherford Appleton Laboratory, Didcot, United Kingdom.
[ll]Also at School of Physics and Astronomy, University of Southampton, Southampton, United Kingdom.
[mm]Also at INFN Sezione di Perugia, Università di Perugia, Perugia, Italy.
[nn]Also at KFKI Research Institute for Particle and Nuclear Physics, Budapest, Hungary.
[oo]Also at Institute for Nuclear Research, Moscow, Russia.
[pp]Also at Horia Hulubei National Institute of Physics and Nuclear Engineering (IFIN-HH), Bucharest, Romania.